University of Oklahoma

Graduate College

INVESTIGATION ON THE EFFECT OF DRILLSTRING STIFFNESS ON DOWNSCALING DRILLSTRING VIBRATIONS

A THESIS

SUBMITTED TO THE GRADUATE FACULTY

in partial fulfillment of the requirements for the

Degree of

MASTER OF SCIENCE

By

JAKE YANCEY

Norman, Oklahoma

2021

INVESTIGATION ON THE EFFECT OF DRILLSTRING STIFFNESS ON DOWNSCALING DRILLSTRING VIBRATIONS

A THESIS APPROVED FOR THE

MEWBOURNE SCHOOL OF PETROLEUM AND GEOLOGICAL ENGINEERING

BY THE COMMITTEE CONSISTING OF

Dr. Catalin Teodoriu, Chair

Dr. Ramadan Ahmed

Dr. Deepak Devegowda

Acknowledgements

I would like to thank Dr. Teodoriu for his assistance in igniting my passion for drilling as well as for all his work assisting me in my studies. Without his assistance, this thesis would not have been possible.

I would like to thank the members of my committee, Dr. Ramadan Ahmed and Dr. Deepak Devegowda for their support and comments on my thesis.

In addition, I would like to thank both of my parents for teaching me as I grew to have a curious mind and strong work ethic. They are the ones who gave me the skills and knowledge to reach as far as I have.

Thank you to all of my friends who have aided me on this journey of higher education. The love and assistance I have received has been invaluable and is what allowed me to finish what I've started.

--- Jake Yancey

Table of Contents

List of Tables

List of Figures

Abstract

Drillstring vibrations provide one of the most important challenges to drilling efficiency today. These vibrations can cause many issues such as decreased energy transfer from the to drive to the bit, fluctuating drilling parameters, and damage to the bit and formation. All of these issues will lead to additional time and money that must be invested in order to drill to the same depth, thereby limiting the wells that can be attempted. One of the most prevalent forms of these vibrations is torsional vibrations or stick-slip interactions. These vibrations occur in approximately fifty percent of drilling done today and thus are the most common type of major vibrations (Dufeyte & Henneuse 1991).

The objective of this thesis was to develop and test a small-scale model of torsional vibrations in order to permit the testing of various parameters and their impact on the occurrence and intensity of stick-slip interactions. By creating a reduced scale model, testing can be conducted in laboratories and for a much-reduced economic burden. Therefore, a 1.6 meter model of a drillstring based upon the Kyllingstad & Halsey (1988) torsional pendulum model was created. This model represents the drillstring in tension above the neutral point. However, in order to induce stick-slip interactions at this scale, steel could not be used. This is because its slip-stick index (SSI) was less than one for all speeds tested. Therefore, other materials must be utilized to allow the stick-slip interactions to occur. Therefore, this thesis compares four strings and their applicability to testing at this scale. These strings were made of aluminum, polyethylene, and nylon.

The method utilized in the testing of the model was to secure each string between a top drive and a brake which represented the torque provided by the formation. The string was then rotated by the top drive while the brake was engaged, leading to a period of time where the top of the string rotated while the bottom remained stationary (sticking). Then, once the torque from the brake was overcome, the bottom began to rotate again (slipping). The period of time that the sticking occurred was recorded and converted to the angle rotated by the top of the string. This value was then utilized to determine the measured shear modulus which was subsequently compared to the known value for the string material.

When comparing the measured shear moduli to the true shear moduli of the string materials, three of the strings had results which mirrored the real world. All of these strings had shear moduli that stayed consistent through various torques and speeds as well as were close to the true value for the material. However, two of the strings, Strings 1 and 3 (made of aluminum and nylon respectively), were restrained by low tolerances for applied torque and speed. This limits the applicability of their results for future testing. However, String 2, made of polyethylene, not only had accurate results but also was consistent over a wide range of speeds and torques. These factors combine to make this string the prime choice for future testing of stick-slip interactions and the effects of various parameters on their occurrence.

Chapter 1: Introduction

1.1 Motivation

The principal goal in oil and gas is the safe removal of petroleum with the lowest cost to the operator. To this end, there are many aspects to be considered including production, completion, and reservoir management but the area that creates the highest cost and risk is the drilling of the well. Thus, the efficiency of the drilling process has a major impact on the viability of a project in the oil and gas industry.

In order to drill a well, three subsystems provide the actions that extend the length of the wellbore. First, the hoisting system controls the weight on bit (WOB) that exerts the force on the formation. Second, the rotary system provides the torque from the top drive to the bit and allows the bit to shear the formation, thereby lengthening the hole. Finally, the circulating system removes the cuttings from the bit and moves them to the surface.

Increasing the efficiency of the drilling system can be accomplished through many aspects such as improved bit-formation interactions, improved mud composition, managed pressure drilling, or crew performance but this thesis focuses on the reduction of drillstring vibration to improve the efficiency.

Excessive drillstring vibrations will cause a loss of efficiency in the transfer of energy from the surface as well as causing potential damage to both the formation and the bottom hole assembly (BHA). These factors will both increase the time and risk of the drilling operation as well as increasing the accumulated cost from the drilling of the well.

1.2 Problem Description

The three variations of drillstring vibrations are axial, lateral, and torsional (Santos et al. 1999). Axial vibrations are variations in WOB with extreme cases resulting in pounding the bit against the formation. Lateral vibrations can cause the drillstring to repeatedly strike against the wellbore, causing significant damage in the process. Torsional vibrations are the most common and occur when the bottomhole rotation speed fluctuates.

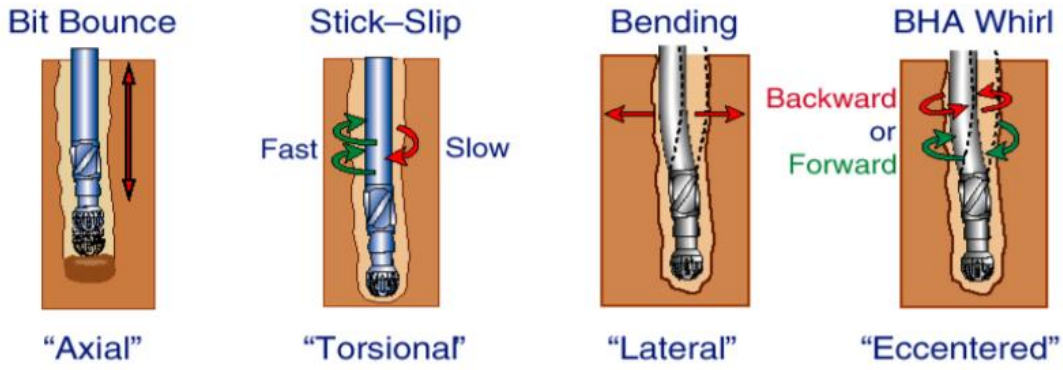

Figure 1: Visualization of drillstring vibrations from Ashley et al. (2001)

Axial vibrations occur in the direction of drilling and most frequently occur in vertical or near-vertical wells with tricone bits, drilling out of the shoe track, or in hard formations (Ashley et al. 2001). It can also be caused through another form of vibrations such as torsional. In addition, these vibrations will often lead to other forms, such as lateral vibrations (Dunayevsky et al. 1993). The indication on the surface is fluctuating WOB measurements. These vibrations are referred to as bit bouncing when the severity results in a loss of contact between the bit and the formation. The impact of

inconsistent weight on bit is a much-reduced rate of penetration (ROP) and therefore increased time drilling. However, in extreme cases such as bit bouncing the repeated shock to the BHA can lead to severe damage and the BHA will need to be tripped out and replaced. In harsh environments such as the igneous environments in the Songliao Basin, these vibrations can combine with other vibrations to cause severe damage and fatigue to the drillstring (Chi et al. 2006). The mitigation for this form of vibration includes reduced aggressiveness while drilling, increasing drillpipe diameter, and soft top drive control (Ertas et al. 2013).

Lateral vibrations and whirl occur when the BHA or the bit rotates eccentrically rather than staying in place laterally. It occurs most frequently in near-vertical wells when proper stabilization is not achieved or in washed out boreholes. These vibrations will usually have twice the frequency of axial vibrations (Besaisow & Payne 1988). This movement results in vibrations that can cause the drillpipe to strike the wellbore, damaging both it and the BHA in the process. In addition, the diameter of the hole drilled will increase and therefore more work will be required to drill to depth. Also, these impacts will increase the surface torque required to drill (Aldred & Sheppard 1992). This increases the time and cost of the drilling process. It also can require tripping out to replace damaged components which further increases the time and cost of drilling. Specifically, backwards whirl produces high bending stresses, especially around joints in the BHA (Aldred & Sheppard 1992). The mitigation of lateral vibrations can be accomplished through anti-whirl bits, additional stabilizers, roller reamers, increased mud lubricity, and correct drilling practices. (Ashley et al. 2001).

The final form of vibrations is torsional vibrations or stick-slip. These vibrations typically occur in “high angle wells, when aggressive PDC bits are used and in environments where the BHA to wellbore friction is high” (Ashley et al. 2001). The cause of these vibrations is a reduction in the rotational speed of the bit due to torque generated by the bit-formation interaction. This reduced rate continues until the elastic potential energy from the top drive overcomes the torque of the formation and the bit is released. The bit will then spin at an increased rate until the friction again slows the rotation. In extreme cases, the bit can completely stop its rotation and then accelerate to over seven times the top drive’s rotation with the minimum speed during slipping being twice the speed of the top drive (Ledgerwood et al. 2010, Kyllingstad & Halsey 1988). Similar to the lateral vibrations, these will have a frequency double that of the axial vibrations (Besaisow & Payne 1988). This form of vibration is detected at surface by fluctuating RPMs and torque. These vibrations can lead to many issues in the drilling process including damage to the bit and formation, over-torquing of connections, and greatly decreased drilling efficiency. The mitigation of these vibrations can be accomplished through a reduction of WOB, increased mud lubricity, reaming, and smoother well profiles. (Ashley et al. 2001).

Because drilling will occur in real world situations rather than in an ideal environment, all of these forms of vibrations will occur at all times. However, they will likely only cause damage to the system and decrease the drilling efficiency if the frequency approaches the resonant frequency of the system (Dareing 1984; Aldred & Sheppard 1992). Changing the frequency to the resonant frequency or a similar value

greatly increases both the occurrence and intensity of the vibrations and the damaging results from them (Spanos et al. 1995). In addition, each drillstring can have as many critical speeds that result in excessive torsional vibrations as there are masses on the drillstring (Brinner et al. 1982).

All of these vibrations are detrimental to the performance of drilling. The primary issue from drillstring vibrations is that energy is dissipated through the vibrations rather than going from the bit into the formation. This leads to a drop in efficiency while drilling and extends the time and energy required to reach the total depth required. Beyond this drop in efficiency, the various vibrations can affect the wellbore and BHA equipment detrimentally. A lack of wellbore stability can result in many harmful situations such as stuck pipe, poor cementation of casing, or even wellbore collapse in extreme cases. In fact, approximately ten percent of non-productive time (NPT) is caused by wellbore stability issues (Krygier et al. 2020). Damage to the BHA assembly will result in lower drilling efficiency and typically will require tripping out of the hole to replace the damaged equipment. Both of these processes take time and will result in unneeded costs. Therefore, the mitigation of drillstring vibrations will improve both the safety and cost associated with drilling for hydrocarbons.

1.3 Introduction to Stiffness

Stiffness is a mechanical property that represents the “force needed to achieve a certain deformation of a structure” (Baumgart 2000). This force, or more accurately load, can occur as a force, moment, or stress applied to the structure. The deformation

that occurs from it is a change in the physical shape of the structure. Generally, stiffness is represented as:

$$Stiffness = \frac{Load}{Deformation}$$

More specifically, rotational or torsional stiffness, *k*, is defined as:

$$k = \frac{M}{\theta}$$

Where, M represents the applied moment and θ represents the rotation. For the SI system as well as this thesis, the unit for applied moment is Newton-meters (Nm) and the unit for the rotation is radians (rads). Thus, the unit for rotational stiffness is Newton-meter per radian (Nm/rad).

For a beam of uniform cross-section, the rotational deformation can be calculated with the equation:

$$\theta = \frac{TL}{GJ}$$

In this equation, θ is the angle of twist in radians, T is the applied torque in Newton-meters, L is the beam length in meters, G is the modulus of rigidity or shear modulus of the material with the unit of pascals, and J is the torsional constant in meters^4 (Higdon et al. 1967).

Some takeaways we can make from this equation are that greater deformation will occur as torque or length are increased. Conversely, it will be reduced when utilizing a material with a higher modulus of rigidity or if the torsional constant is increased. While drilling, the length cannot be shortened while still reaching the desired total depth and the torque applied must be high enough to successfully shear the rock from the

formation. Therefore, if the goal is reducing deformation to increase drilling efficiency, the material of the structure, in this case the drillpipe, should be changed to one with a higher modulus of rigidity. Alternatively, the torsional constant can be increased.

The modulus of rigidity is defined as the ratio of shear stress to the displacement per unit sample length (Higdon et al. 1967). This is a mechanical property of a material and measures the elastic shear stiffness of the material. The unit for this measurement is pascals although it is typically expressed in gigapascals. This value has been experimentally determined for many materials including the materials tested for this thesis. As a mechanical property of a material, this value will not change with the scale of the structure.

The torsional constant is a geometric property of a structure's cross-section that describes the structure's torsional stiffness when combined with material and length. It is a function of the structure's cross-sectional area and its shape that is equivalent to the second moment of area normal to the section (Duleau 1820). However, this only applies perfectly to circular cross-sections due to the assumption that a plane section remains planar after twisting, which is only true of circular cross-sections due to the warping that takes place during deformation. However, approximations have been made for other shapes that can serve the to approximate the torsional constants of these cross-sectional shapes. In addition, because pipes are formed from two concentric circles in the cross-section, the theory will prove true and applicable for them. The equation most applicable to this thesis's calculations is the equation for the torsional constant of a pipe formed by two concentric circles (Higdon et al. 1967):

$$J = \frac{\pi}{32} * (OD^4 - ID^4)$$

This equation was utilized in the calculations of this thesis to determine the torsional constants of the various strings examined as they all were pipes of concentric circles. This equation shows that the ways to increase the torsional constant are to increase the outer diameter of the pipe or decrease the inner diameter. This will be true regardless of scale or material as the equation only relies upon the cross-section of the structure. In addition, because of the circular structure of the pipes, this equation will be exact rather than an approximation.

Stiffness is important in the study of drillstring vibrations because it will influence both the occurrence and intensity of the vibrations, particularly of the torsional variety. Few studies have specifically examined the effect of increasing drillstring stiffness although those that have found that an increase in stiffness will decrease the instances of stick-slip and provide a more efficient transfer of energy from the top drive to the bit, resulting in higher ROP. However, when testing at a small scale such as this experiment did, the high modulus of rigidity of steel can prevent the occurrence of stick-slip interactions. Therefore, materials of a lower modulus of rigidity are necessary for testing (Patil & Teodoriu 2013; Patil 2013). In order to determine if stick-slip interactions will occur, the stick-slip index (SSI) must be greater than one. If the SSI is between 0.5 and 1, torsional vibrations will occur and if the SSI is between 0 and 0.5, weak torsional vibrations will occur (Patil 2013). The equation to determine the SSI is:

$$SSI = \frac{RPM_{maximum} - RPM_{minimum}}{2 * RPM_{average}}$$

The value for the SSI does not vary linearly with increasing RPM. The result will vary by material construction and the speed of rotation. Figure 2 below shows the value of SSI for various string materials:

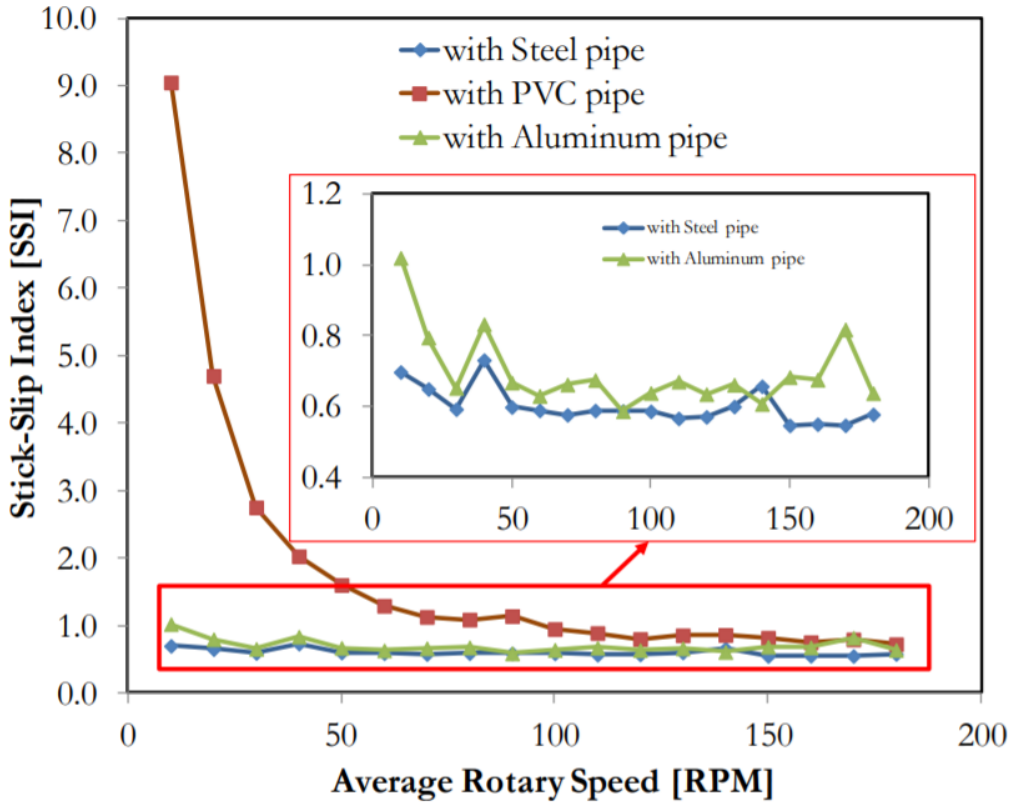

Figure 2: SSI vs Rotary Speed based upon string material (Patil 2013)

According to Patil (2013), stick-slip interactions will only occur with aluminum at very low rpms and will never occur with steel at the small scale. Because the dynamic effects are what this study focuses on, testing at low rpms is undesirable. Real-world drillstrings operate at well over 100 rpms. The only material from Figure 2 that still has

stick-slip interactions occurring at 100 rpms is the PVC, therefore influencing the choices of materials to test for this experiment.

The stiffness of a 5.5 inch, 21.9 lb/ft drillpipe per meter can be calculated with the shear modulus times the torsional constant. In the case of this drillpipe, the value is $1.24*10^7$ Nm^2/rad. As the shear modulus does not change with various drillpipes as they are all made of steel, the way to increase this value is to increase the torsional constant by increasing the outer diameter or by lowering the inner diameter.

1.4 Goals of the Experiment

This experiment was conducted in order to determine whether the constructed drilling model could provide results with real world applications. These results were specifically related to the occurrence and prevention of stick-slip interactions at the bit. Thus, this experiment recreated stick-slip occurrences in the scale model. This data was then analyzed to determine if the interactions and their effect on the system as a whole followed the real-world results. The metric to determine this was whether the results of the experiment had constant or near constant values for the modulus of rigidity. In theory, this value is a material property and as such should not change based upon the tests and their conditions.

The second goal of this experiment was to determine if any of the string sizes and materials tested provided superior results when testing stick-slip interactions. The use of a steel string would not have worked because of the limitations of the experimental setup. Under static conditions the stiffness depends strictly on the

material properties and it is a very important parameter for the stick slip phenomenon which is actually a dynamic process. As such, if a system needs to be downscaled for dynamic investigations, geometrical downscaling factors may not be sufficient, and thus stiffness needs to be adjusted. This is possible only through material changes.

Determining whether a string provided accurate and reliable results could be determined through both objective and subjective metrics. First, the material should behave in such a way that the measured modulus of rigidity remains relatively constant throughout testing at various speeds and values of applied torque. Second, this material should provide data over a wide range of experimental conditions and not create any additional errors that must be accounted for in the analysis of the results.

Chapter 2: Current Research

2.1 Analytical Models

There has been much research done on the topic of drillstring vibrations and their effects through the years. One of the first examples of this research was Dareing and Livesay (1968). This thesis created a model that describes the drillstring as a pendulum suspended by a spring representing the hoisting system. This model, shown below in Figure 3, accurately demonstrated longitudinal and angular vibrations but did not touch on torsional or longitudinal vibrations. It also did not fully account for the friction inherent in the real-world drilling system as it assumed that the viscous friction of the model represented all of the various types of friction in the real system such as fluid, rubbing, and material.

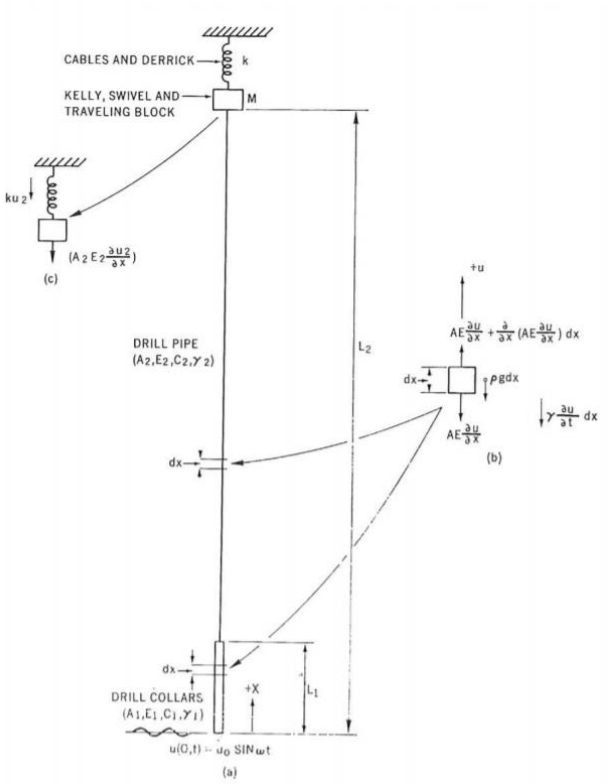

Figure 3: Drillstring Model from Dareing and Livesay (1968)

Other studies followed that focused more on the aspects that had heretofore been neglected. Kyllingstad and Halsey (1988) created an analytical model for stick-slip motion of the bit also known as torsional vibrations. This model describes the drillstring as a torsional pendulum and assumes that there is limited twisting in the stiffer BHA and it is therefore treated as a flywheel for the model. This mathematical model predicts that the speed of the bit as it releases from the stick of the formation is always more than twice as fast as the surface speed, supporting the analytic data from Besaisow & Payne (1988). This model also assumed a viscous dampening of the vibrations in its calculations. In addition, this model places a good bit of importance in reducing the occurrence of stick-slip interactions on the stiffness of the drillstring because the increased stiffness can work to prevent the propagation of vibrations. Through this model, the prediction of top torque was conducted and found to be linearly increasing at high RPMs. This model was tested in the laboratory in Lessley et al. (2017). Through the use of this physical testing, it was determined that the model accurately predicted the decrease in stick time with increased rotational speed. However, the new testing showed that the effects of density on the duration of stick-slip were low while the shear modulus was much more significant as it followed a logarithmic relation.

As drilling shifted to include more deviated and horizontal wells, the requirement grew for models that predicted vibrational behavior in the horizontal. Even though the vibrations in the horizontal are less intense due to the fact that energy can be more easily dispersed through the formation, the vibrations are still present and can cause damage to the formation and BHA. The complexities added to a horizontal system

when compared to a vertical are that additional forces are exerted on the side of the drillstring as well as greater friction from the interactions between the BHA and the formation. Omojuwa et al. (2012) created a new model to simulate the drillstring in these conditions as shown below in Figure 4. Based upon this model, predictions could be made on the deformation of drillstrings and the generation of torque from the formation. As torque on the BHA from the formation is one of the main causes of stick-slip interactions, this model can provide insights into how to reduce their occurrence.

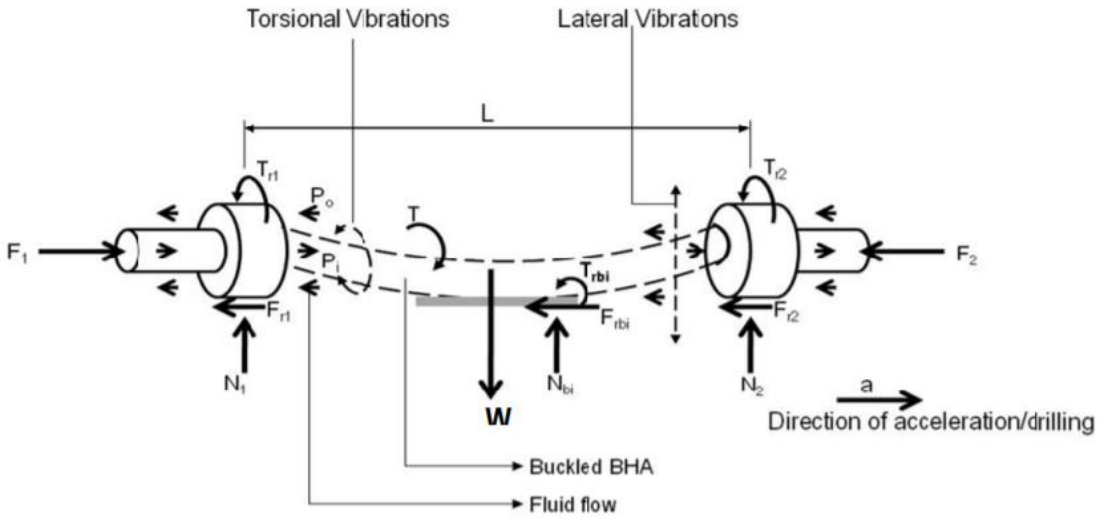

Figure 4: Model of horizontal drillstring created by Omojuwa et al. (2012)

Specifically regarding the occurrence of stick-slip interactions, Patil & Teodoriu (2013) developed a new analytical model to investigate the effect of various parameters on the occurrence of vibrations. Again designed as a torsional pendulum, this model represented the variation in stiffness between the BHA and drillpipe by utilizing two springs of differing stiffnesses. From this model, a number of parameters were adjusted and the resulting changes in stick-slip and ROP were observed. Namely, the parameters were surface rpm, WOB, drillstring stiffness, drillstring inertia, and the confined

compressive strength of the rock. The study found that increasing the surface rpm resulted in reduced stick-slip occurrences and increased ROP. WOB was found to greatly increase the occurrence of stick-slip although ROP was also increased, at least until buckling began to occur in the drillstring. Drillstring stiffness was found to reduce stick-slip and ROP. However, because the modulus of rigidity for steel is constant, this implies that the cross-sectional area of the drillpipe was increased, thereby increasing the drillstring inertia. In a vacuum, this increase in inertia was shown to have the opposite effect where bit stoppage increased and the ROP decreased due to the additional mass to be rotated. Finally, the confined compressive strength of the rock was shown to decrease ROP.

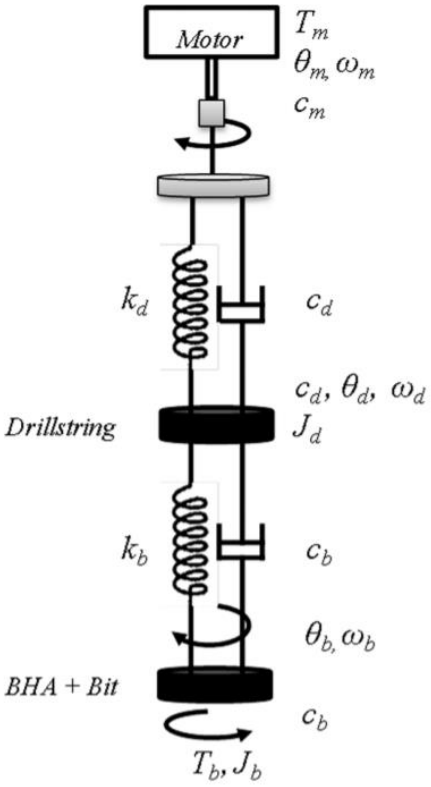

Figure 5: Double Pendulum Model from Patil & Teodoriu (2013)

2.2 Physical Models

Westermann et al. (2015) developed a scaled drillstring model to test the impact of lateral vibrations within the BHA. This model was designed to represent only a small section of BHA rather than the entire length of the drillpipe as it would otherwise become impractical. The stiffness of the rest of the drillstring is simulated through the use of a spring attached to the end of the setup. It is a lateral setup to represent the BHA in a horizontal well. The setup is designed to measure both lateral and torsional vibrations caused by drilling although the results of the experiment only discuss the lateral vibrations. It is also notable for being able to measure the lateral forces applied to the system which does not occur in the majority of physical models. However, this setup does neglect to measure the effect of stiffness on the appearance of torsional vibrations and stick-slip interactions.

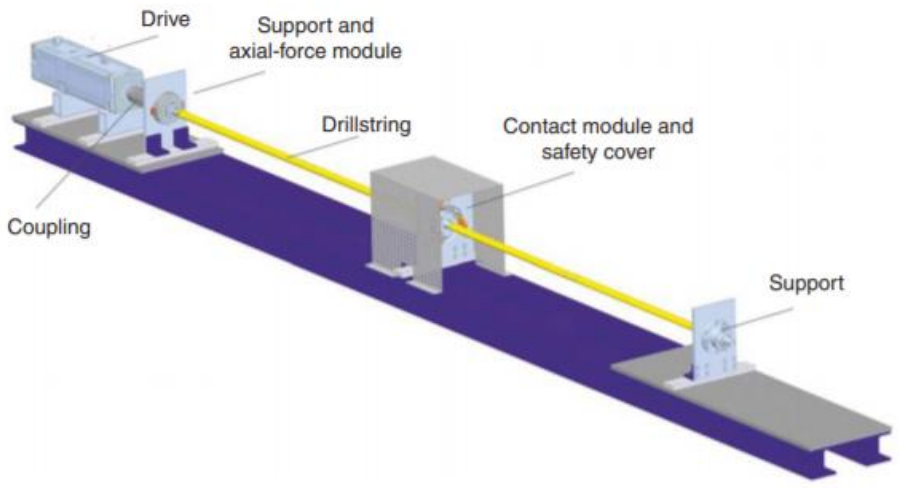

Figure 6: Scale model utilized in Westermann et al. (2015)

Esmaeili et al. (2012) created a scale model to measure string vibrations while physically drilling through rock. The inclusion of physically drilling a hole in the

laboratory is novel although it does mean that the test simulates the lower BHA much more than the entire drillstring. The goals of the experiment were to confirm the effects of varying various parameters on the ROP and occurrence of vibrations. Specifically, this experiment examined the effects of rotary speed and WOB. The results confirmed much of what the analytical models had predicted. Increasing the rotary speed increased the ROP of the system as well as the occurrence of vibrations. WOB also produced the expected results with an increased ROP although the impact on the occurrence of drillstring vibrations was not major. It is important to note that the vibrations tested were of the lateral variety and thus this experiment did not go into the occurrence of stick-slip vibrations.

Figure 7: Experimental setup for Esmaeili et al. (2012)

Sharma et al. (2020) describes the creation and use of a small-scale string model of a scale much larger than most other models created. This model has a length of 15 meters. This scale as well as the sensors utilized allow precise control of many aspects that are much more difficult to simulate at the smaller scale already examined. For example, because the diameter can be better controlled at higher scales, materials that more closely resemble the steel of a true drillpipe can be utilized. This experimental

setup has been utilized to generate and study the effects of rpm on the occurrence of stick-slip interactions. It also has been shown to provide good repeatability between tests, indicating the data should reliably represent the true interactions.

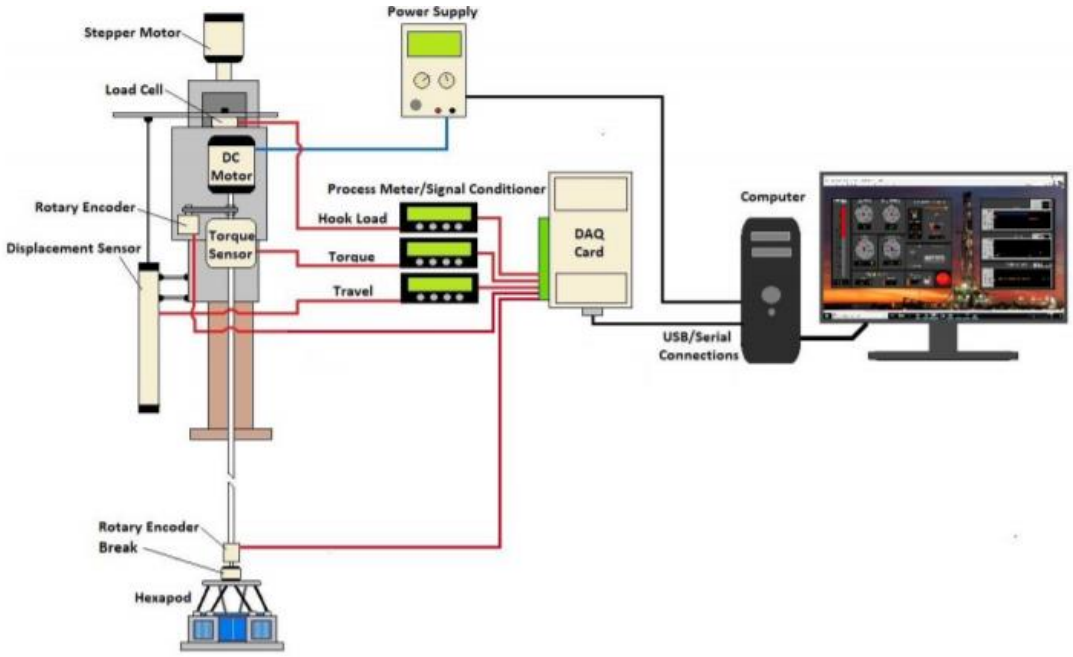

Figure 8: Main components of the Sharma et al. (2020) setup

Chapter 3: Downscaling for Experimental Setup

3.1 Reasons for Downscaling

Because experimental data from the real world is preferable to purely theoretical data due to their increased reliability, testing should be conducted on a physical model. However, testing on a full scale is neither practical nor economical due to the requirements for both land and drilling equipment. Therefore, a reduced scale to be utilized for testing that can be constructed at a low cost as well as at a practical size is important for further testing.

3.2 Law of Similitude

When attempting to create a scale model, it only has similitude with the real application if it shares geometric similarity, kinematic similarity, and dynamic similarity. However, because drillstrings are many thousands of feet long, a model directly scaled geometrically would not be feasible for the dimensions of the components such as the drillpipe. This is because the materials would be so thin that they could not provide the same inertia and stiffness properties as well as becoming difficult and expensive to source. Therefore, substitutions of materials must be done in order to provide proper kinematic and dynamic similarity. For the purposes of this thesis, dynamic similarity is the issue focused on in the selection and testing of string materials. To this end, the three critical parameters for the string materials and sizes are the angular deflection generated, the maximum applied torque before buckling or damage occurs, and the torque that provides usable results for testing.

3.3 Downscaling Factor

In order to determine the downscaling factor of the experimental setup, the length of the small scale string must be divided by the length of the real world drillstring in the equation:

$$n = \frac{L_{scale}}{L}$$

Where n is the downscaling factor, L_{scale} is the length of the small scale string, and L is the length of the real world drillstring. However, this downscaling is not practical as it will result in outer diameters of strings that are unavailable and would be very fragile. Therefore, the alternative method of upscaling the available materials to an equivalent real-world scale would be to scale the capabilities of the drillstring and specifically its stiffness. The stiffness of a structure is defined as:

$$\frac{GJ}{L} = \frac{T}{\theta}$$

Where G is the modulus of rigidity, J is the torsion constant, L is the length of the structure, T is the torque applied to the structure, and θ is the angle of deformation in the structure. By scaling the stiffness rather than the physical size of the model, the practicality of the design is greatly increased. It allows the direct comparison between the model's results and the real world while still maintaining the use of common materials and sizes.

The scaling of stiffness would be defined by the equation:

$$n = \frac{G_{scale}J_{scale}}{GJ} = \frac{G_{scale}}{G}\left(\frac{OD_{scale}^4 - ID_{scale}^4}{OD^4 - ID^4}\right)$$

Where n is the scaling factor, G_{scale} is the modulus of rigidity for the model string, G is the modulus of rigidity for the real-world drillstring, J_{scale} is the torsion constant for the model string, and J is the torsion constant for the real-world drillstring,

This equation was utilized to determine the scaling of the strings compared to the real world drillstring. The decision of what materials and diameters of string substitute to utilize in the testing was generally governed more by availability than by the physical similarity of dimensions and thus a general equation like this one that can relate the two scales proved to be invaluable in the generalizability of the miniature strings.

When comparing the scaled strings to the true drillstring, a standard value for the real-world drillstring was required. The final decision was to compare the results with a 5 ½ inch drillpipe with a nominal weight of 21.9 lbs/ft. This means that the OD was 13.97 cm and the OD was 12.13 cm. These values were then compared with each string to determine the scaling factor, as will be discussed in section 4.2.

Chapter 4: Experimental Design

4.1 Physical Model

The setup that this experiment was conducted on is a model of a vertical wellbore that has a string length of approximately 1.6 meters. The experimental setup is shown below in Figure 9:

Figure 9: Entirety of physical experimental setup

The setup was constructed on a base material of plywood to provide the structural support to the device. To this structure was vertically attached a metal rail to allow for adjustment of the length of the setup to the length of the string. At the top and bottom of this rail were two sleds that housed the components to be utilized for the testing as will be described below.

Figure 10: Top sled containing rotary encoder and stepper motor

The top sled as pictured above simulated the top drive of the real-world drilling rig. The gray and black cuboid in the center of the image is the stepper motor. This stepper motor provided the power and torque to the system during the experiments. Stepper motors operate by completing a full rotation as a number of small steps. This model completed a single rotation in 200 steps. Above the stepper motor at the top of the image is a rotary encoder. This device operated to record all the data for the experiment. It recorded the speed, direction, and position of the top of the string. It operated at a rate of 10 Hz which means that it collected data 10 times per second or

once every tenth of a second. Below the stepper motor at the bottom of the image is the bracket that held the top of the string. This was removable in order to replace the strings for testing the various sizes and materials.

Figure 11: Brake and bottom rotary encoder

Figure 11 shows the setup of the bottom sled. This sled is designed to simulate the interaction of the bit and formation. To this end, there is a hysteresis brake attached near the top of the image to provide the requisite torque. A hysteresis brake operates by utilizing an electric current to generate an internal flux that provides constant drag to the attached shaft. This torque will thus vary with applied current. Figure 16 shows the

values of torque vs current for the particular brake utilized in this experimental setup. Below the brake is another rotary encoder identical to the one at the top of the string. Just like the other encoder, this one operates at a frequency of 10 Hz and records the speed, direction, and position of the bottom of the string. Again, in a similar vein to the top of the string, a removable bracket attaches the bottom of the string to the sled to allow for the changing of strings for various tests.

Figure 12: Power supply to the brake at bottom of string

The current for the hysteresis brake was provided by the power supply shown in Figure 12. This particular power supply could be connected to a computer to run a

program to turn it on or off as well as control the amperage and voltage. However, the maximum amperage the system could run at was capped at 0.150 A, thereby limiting the range of torques that could be produced by the brake.

Figure 13: Two Arduino boards operating to control motor and record sensor data

Figure 13 above shows the Arduino boards that operated the stepper motor and recorded the data from the sensors. The first Arduino ran a program controlling the stepper motor in terms of speed and total number of steps, which translates to the length of time that it is operating. The second Arduino board translates the data from the sensors into time, rotation speed, direction, and position and transfers this data to a computer to allow it to be recorded and analyzed.

4.2 Strings and Their Properties

For this experiment, four strings were tested in the experimental setup described above. These strings were made of multiple materials and sizes and allowed the test to see results from all ends of both stiffness and size. They fell into two categories, namely the thicker and thinner strings.

The first string to be tested was made of aluminum. It followed the shape of a hollow pipe so as to best simulate the drillpipe it was based upon. The outer diameter was 3.22 mm and the inner diameter was 2.43 mm. The length of the material was 1.66 m. Of all the materials tested in this experiment, aluminum was the one with the highest modulus of rigidity or shear modulus. Aluminum's modulus of rigidity was 27 GPa which means that for the same cross-sectional area, it would provide the greatest resistance to deformation (Engineering Toolbox). The downscaling factor for this string is $1.55 * 10^{-8}$.

String 2 was made of polyethylene. It again had a pipe's cross-section of concentric circles. The outer diameter for this string was 9.23 mm and the inner diameter was 4.20 mm. The length of this string was 1.547 m. This was the thickest of the strings tested. The material provides a much lower modulus of rigidity than the aluminum of String 1. However, polyethylene has a wider range of values as the exact composition and construction method can vary. The modulus of rigidity should be in the range of 0.12 GPa to 0.21 GPa meaning that it will resist deformation at a much lower rate than the aluminum of String 1 (Engineering Toolbox; Laminated Plastics). The downscaling factor for this string is $6.59 * 10^{-9}$.

String 3 was made of nylon. This string was not in the shape of a pipe but instead had a cross-section of a simple circle with a diameter of 1.55 mm. The length of this string was also 1.547 m. The modulus of rigidity for nylon is 4.1 GPa which is between the values for polyethylene and aluminum. However, as this string had a much smaller cross-section, it still had a much smaller stiffness than the previous two strings (Engineering Toolbox). This was the first of the thin strings and served to provide the low end of the testing range. The downscaling factor for this string was $5.48*10^{-12}$.

String 4, the final string tested, was again made of polyethylene. Similar to the thick strings, this string had a cross section of concentric circles with an outer diameter of 3.12 mm and an inner cross-section of 1.8 mm. The length was 1.574 m. The expected value for this string's modulus of rigidity is again between 0.12 and 0.21 GPa (Engineering Toolbox; Laminated Plastics). Notably, while made of the same material, this string displayed much more flexibility than the previous strings and was the most likely to buckle. The downscaling factor for this string was $8.37*10^{-11}$.

String	String 1	String 2	String 3	String 4
Material	Aluminum	Polyethylene	Nylon	Polyethylene
Modulus of Rigidity (GPa)	27	0.12-0.21	4.1	0.12-0.21
Length (m)	1.66	1.547	1.547	1.574
OD (mm)	3.22	9.23	1.55	3.12
ID (mm)	2.43	4.2	0	1.8

Table 1: Strings and their properties

4.3 Experimental Design

In order to conduct the experiment, the strings were first placed into the setup described above. These strings were then tensioned so as to remove any slack from the system. This simulates the effects that are felt by the string above the neutral point rather than the BHA. Please note that the lengths were measured while the strings were under tension and thus under the experimental conditions.

To begin the experiment, with the sensors recording their requisite data, the stepper motor began to rotate at the appropriate rate of rotation. At this point, the brake was deactivated so that there was no torque at the bottom of the string other than friction. The bottom was allowed to spin without the brake's torque until it matched the rate of rotation of the top of the string. This meant that the slack had been removed from the string and the test was ready to begin.

At this point, the power supply was activated so that it provided the requisite current to the brake. This led to an immediate increase in torque on the system and stopped the motion of the bottom of the string, simulating the sticking of the bit on the formation. Throughout this process, the stepper motor and thus the top of the string has continued to rotate at the same rate. This simulates the continued rotation of the top drive while drilling. The elastic potential energy thus built up in the string until it overcame the torque provided by the brake. Therefore, the bottom began to rotate again and thus simulated the slip of the stick-slip interaction.

From this point, the testing would vary depending on the string being tested. The thicker strings, after overcoming the torque in the brake, would continue to rotate at

the same speed as the top of the string. Therefore, no more stick-slip would be observed. Because of this, the current to the brake was cut. This removed the torque on the bottom of the string and the string released its built-up elastic energy. The top of the string would continue to rotate and again remove the slack from the string. After this was achieved, the brake would be reengaged. This would initiate another stick-slip occurrence and the data would be logged. This process was repeated until all the requisite data was acquired.

The thinner strings provided an additional challenge in their testing when compared to the thicker ones because of their comparatively low stiffness. For these strings, stick-slip would occur even when the brake was deactivated. Therefore, the resetting of the string by releasing the torque form the brake was not effective. In fact, it became very difficult to determine when examining the stick-slip occurrences whether the brake was activated or not. Because of this, the testing for the thinner strings was conducted by leaving the brake continuously on. This did not eliminate the occurrence of stick-slip interactions like it had in the thicker strings and as such allowed the testing of the thinner strings to continue as well as producing more data points for the same amount of experimental time.

The strings were each tested at three torque values, which varied based upon the string properties. These tests were conducted at 10, 20, 30, 40, and 50 rpms. This resulted in a total of fifteen tests for each drillstring and a total of sixty tests.

4.4 Assumptions in the Experimental Setup

In the analysis of the data from this experiment, certain assumptions needed to be made. First, the assumption was made that the brackets and attachments of the strings to the sensor, motor, and brake had negligible bending when under torque. This assumption means that the bending measured by the system was exclusively originating from the strings themselves. Next, it was assumed that the stepper motor maintained a constant speed of rotation rather than making many steps at a high speed followed by a period of stopping. However, due to the data collection rate of the sensors on the setup, this assumption plays little role as any variation is undetectable. It was also assumed that the stepper motor rotated at exactly the speed that was programed into it, namely exactly multiples of 10 rpm. Also, because of variations in the data recorded, it was assumed that any slight rotations while the sticking was occurring were errors in the sensors and did not indicate that slip had occurred. The value for “slight rotations” varied with the rpm of the top drive because errors of a greater magnitude occurred at the higher rpm values. Another assumption in this experimental setup is that the strings did not experience any buckling that would change their shape and other properties. In addition, the assumption was made that the friction in the system would be the same for all strings during their testing. The real-world drillstring was also assumed to act as a pipe of constant diameters and thus ignored connections. Finally, it was assumed that the modulus of rigidity was equivalent for both static and dynamic forces.

Chapter 5: Results

The data that was collected from all the sensors during the experiments were the number of ticks (equivalent to time), the direction of the motor's rotation, the speed of the motor's rotation, the position of the motor, the direction of the bottom of the string's rotation, the speed of the bottom's rotation, and the position of the bottom in its rotation. In addition to this, the inputs of amperage to the electric brake and the intended speed of the motor were known.

The data that was most applicable to this experiment were the time and speed of the bottom string's rotation. Because the data collection was done at a rate of 10 Hz, each tick of data is equivalent to a tenth of a second passing. Therefore, by starting at time=0 and adding 0.10 seconds per tick, the equivalent time can be calculated. These values were then utilized to determine the length of time that stick-slip occurred.

The bottom speed was the data utilized in determining the presence and duration of stick-slip. To accomplish this, the values were examined from when the brake stopped the rotation until the bottom began to rotate again due to the buildup of potential energy. The number of ticks were then added up and multiplied by 0.10 in order to find the length of time that the stick-slip occurred.

Figure 14 shows the bottom rotation speed of the string as well as the time that each data point occurs at. The methodology for determining where stick-slip was occurring is to find where the rotation is zero. However, due to errors in the measurements, all data points that were close to zero were assumed to represent sticking. This error occurred more often with higher RPMs. The end of the sticking

period was determined as when the rotation resumes. This resumption of rotation will occur with a speed of rotation much larger than the top's rotation speed, sometimes up to seven times larger.

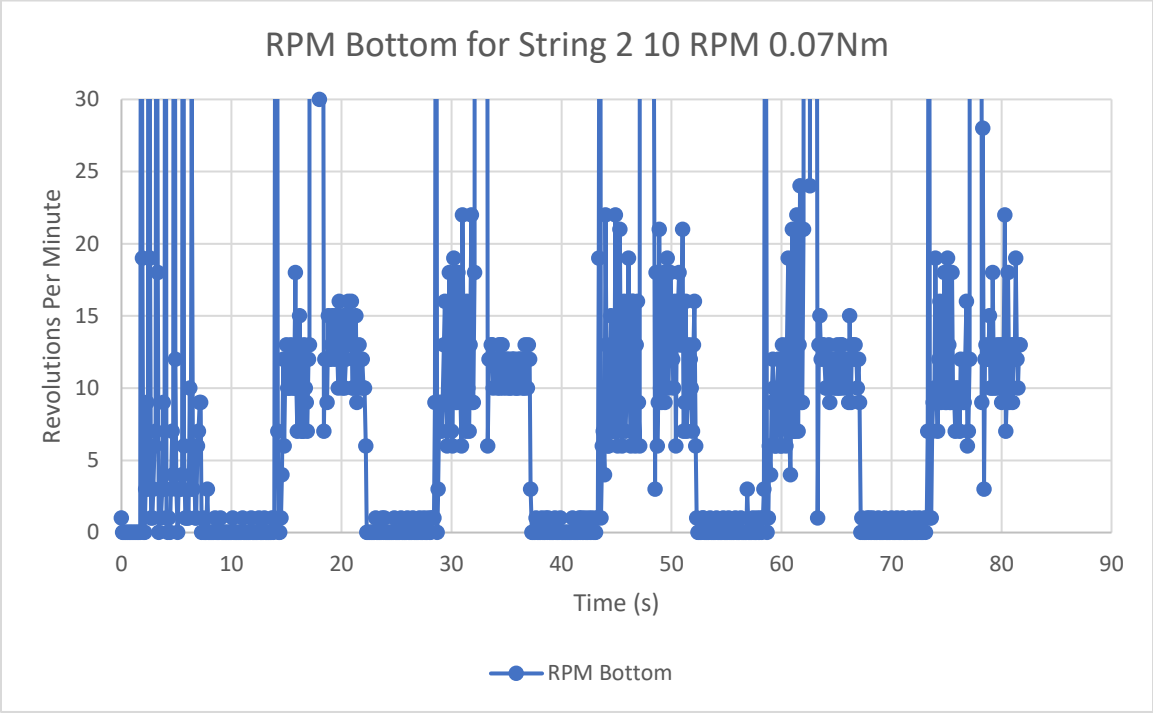

Figure 14: Rotational speed at each time for the bottom of String 2 at 10 RPM and 0.07 Nm

Figure 14 above shows an example of the data from one of the thick strings. This utilized the technique of turning the brake on and off as described above. The dropping of the rotation to zero occurs only when the brake is activated for these strings due to their relatively high stiffness. There is then a spike afterwards once the elastic potential energy is built up to the point that it can overcome the torque provided by the brake and by the system's inherent friction. The brake is subsequently released which results in a short period of erratic motion in the bottom of the string. This is allowed to

dissipate and reach a stable level which is shown in the period before the next occurrence of stick-slip.

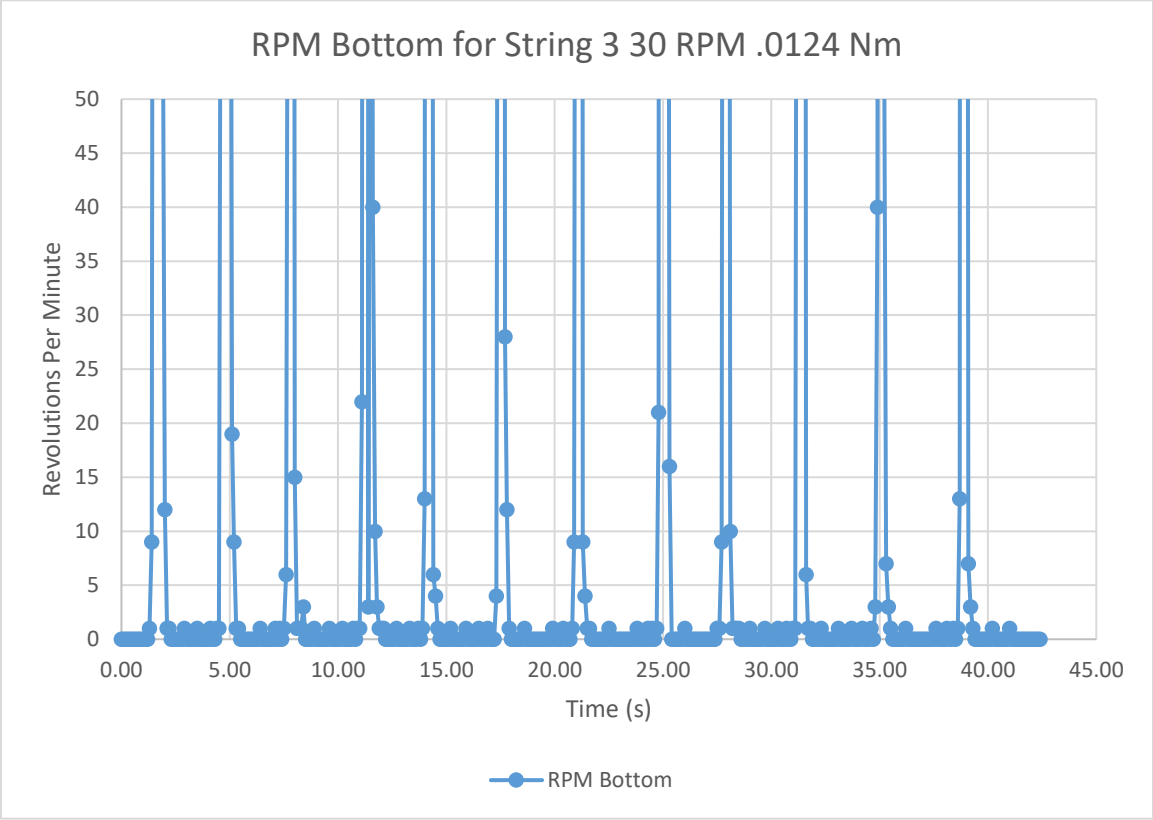

Figure 15: The revolutions per minute of the bottom of String 3 at 30 rpm and .0124 Nm of torque

As discussed above, the thin strings could not be tested in the same manner as the above strings as their reduced stiffness resulted in stick-slip occurring regardless of whether the brake was activated, leading to inconsistent data when the previous methods were utilized. Therefore, the brake was kept on rather than switched on or off. The length of time that the stick occurred was measured in the same manner as with the previous experimental design. However, as demonstrated above, more occurrences

of stick-slip occurred for the same length of test, resulting in more data points for these strings.

Table A.1 shows the data obtained for String 1. The data shown is the length of time in seconds of the recorded sticking as well as the conversion to degrees and radians. Below each set of data is the average value obtained for each rotational speed as well as applied current. The data shows that the results are relatively consistent within each set. In addition, there is an increase in sticking time as applied torque increases which is consistent with the expected results. Due to the tick rate of the rotary encoders, the data for speeds above 30 rpm was unusable.

Table A.2 shows the data from the String 2. This string allowed data analysis at all rates of rotation up to 50 rpm. In addition, it was able to operate at a much greater range of torque values than the aluminum. Similar to String 1, the data on this string is relatively consistent within sets with the exception being the data obtained from the tests at 10 rpms. This is a known problem with the rotary encoders at low speed. The consistency at other speeds implies that this error lies with the sensor error rather than with the string itself.

Table A.3 shows the data from String 3 between its various tests. This string had the least consistency within its sets as the variation reaches forty percent during testing at 10 rpms. This factor leads to uncertainty in the results from this string. However, the values do follow the expected trend of increased time/rotation with increased torque so the overall average at least remains in the predicted pattern. It is also important to mention that the testing methodology was altered to reflect the properties of the

thinner strings. As mentioned above, this string was subjected to constant torque rather than the intermittent torque provided to the thicker strings. This led to the increased number of datapoints as seen in the table.

Table A.4 shows the data for String 4. This string, similar to String 3, was on the thinner end of those tested. This means that the testing methodology changed to reflect the properties of the strings and many more datapoints became recordable. However, this also resulted in a more inconsistent number of results as can be seen in the difference in number of results per set at the same rpm. However, again with the exception of the 10-rpm data, the sets are internally very consistent. This indicates that the results should be accurate to the string undergoing testing.

Chapter 6: Analysis and Discussion

6.1 Description of Analysis

Due to the tick rate of the sensors being limited to 10 Hz, the data from each run cannot be analyzed on its own as it is not precise enough to be usable. For example, at 30 rpms, String 1 would have sticking times of 0.10 and 0.20 seconds. Therefore, the analysis of this speed and string would result in variations of 100%. Instead, the data for each string at each rotational speed and torque value must be averaged. This will give a value between the tenth of a second precision of the sensors and provide a more accurate result.

Because the equation used to determine the validity of the results utilizes the total rotation of the top of the string rather than the time it was spinning, the units must be converted. Specifically, the conversion must be from seconds to radians. This conversion was accomplished through a simple conversion based upon the speed of the top of the string in revolutions per minute shown below:

$$\theta = T * \frac{RPM}{60} * 2\pi$$

Where θ= angle traveled by the top of the string in radians, T= the time in seconds of sticking, and RPM= the revolutions per minute that the top of the string was travelling at.

The next value to be determined is the torque on the bottom of the string. This value can be found through the comparison of the current and the torque provided by the hysteresis brake as shown in the Figure 16 below:

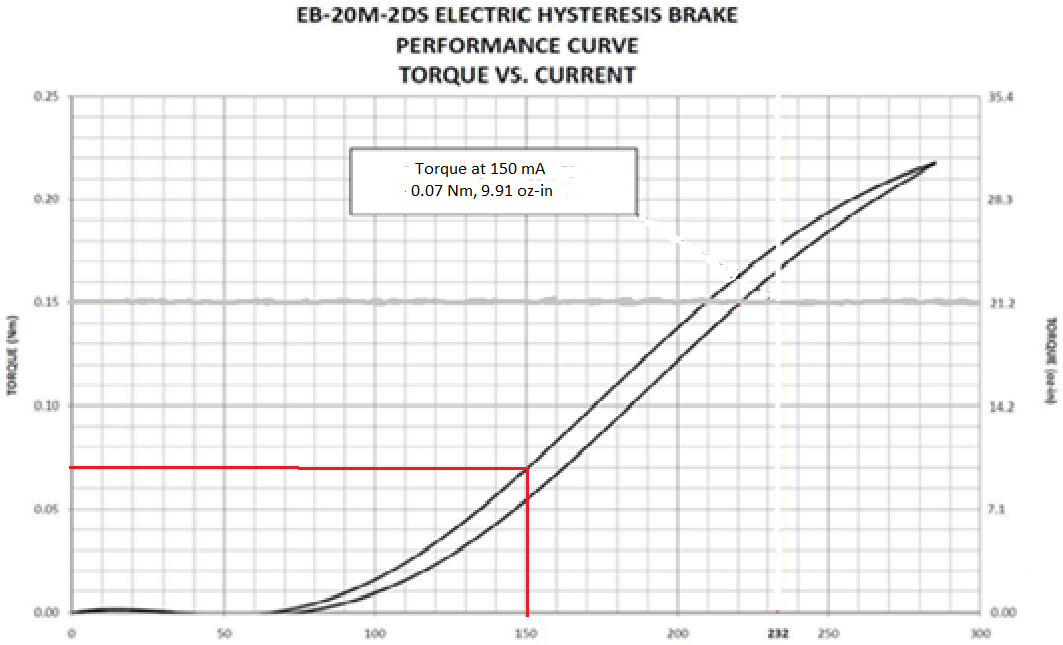

Figure 16: Torque provided by hysteresis brake vs current provided from power supply

Aspects of this chart are not entirely accurate in the data provided. Specifically, this chart shows a decrease in torque from 20 to 50 mA of applied current. In practice however, the torque experienced by the thinner strings increased during this range of currents. This can be ascertained because the same material had a longer stick time at the same rpm with additional the current. This is due to the presence of additional torque. Therefore, the values of torque for the thinner strings must be estimated, increasing the error associated with their results.

The next calculation necessary for analysis was the calculation of the torsion constant, J. As discussed in section 1.3, this equation is based upon the cross-section of the structure undergoing bending. For the case of pipes made of concentric circles, the equation for J is:

$$J = \frac{\pi}{32} * (OD^4 - ID^4)$$

Where J = the torsion constant in meters^4, OD= outer diameter in meters, and ID= inner diameter in meters. This equation also works for cross-sections of a solid circle where the inner diameter is simply zero. With this value as well as θ calculated, it can now be plugged into the following equation to determine the measured modulus of rigidity:

$$G = \frac{T * L}{J * \theta}$$

Where G= the modulus of rigidity in Pascals, T= the applied torque on the bottom of the string in Newton-meters, L= the length of the string in meters, J= the torsion constant in meters^4, and θ= the rotation of the top of the string in radians. This value is known for the materials tested and therefore the data can be compared to this known value to determine the accuracy of the results. In addition, this value should be constant in all conditions as it is a property of the material of the string. Thus, the results from the experiment should result in a near horizontal line.

6.2 Results by String

The first string analyzed was String 1, the aluminum string. This string provided the most confidence in testing because the value of aluminum's modulus of rigidity is more precisely known because it varies less in the various construction methods. Thus, this material would provide the benchmark for our testing.

While all strings had been tested at 10, 20, 30, 40, and 50 rpms, the results from the highest values of rpm had to be discarded for certain strings as the data became unusable at these speeds. This was because the length of time that the stick was

occurring was low enough that it was either undetectable by the sensors or was only detected as a single tick. Aluminum fell into this category as the precision of the sensors was too low to give usable values for the length of the stick above 30 rpm. Therefore, all analysis on String 1 was done on the three lowest speeds.

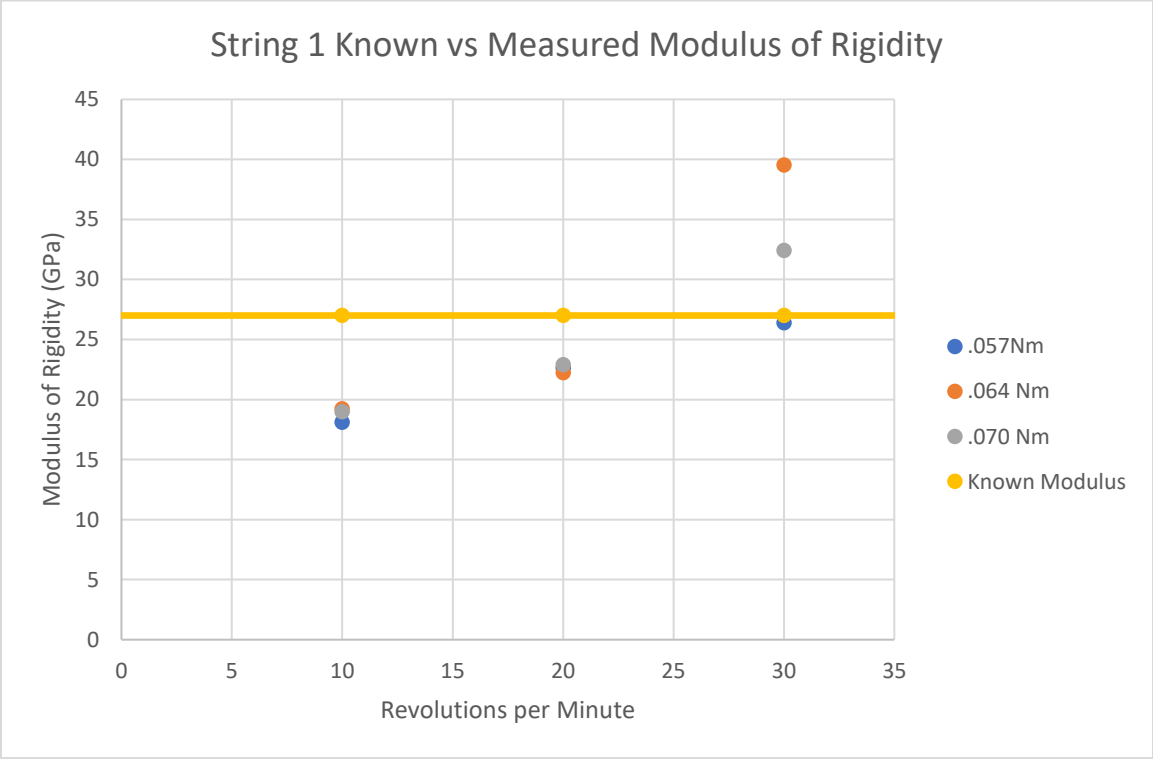

Figure 17: String 1 modulus of rigidity vs revolutions per minute.

Figure 17 above compares the modulus of rigidity that was calculated from the measured values with the known value for aluminum alloys. Regardless of the value of torque or rotational speed, this value should be equivalent. This assumes that the modulus of rigidity remains stable for both static and dynamic operations. The main concerns with this data are that the trends are relatively consistent in value and that the data points follow each other regardless of torque. In this case, that is true, particularly at 10 and 20 rpm. While the data does begin to separate at 30 rpm, it is likely due to the

low tick rate of the sensors. Unfortunately, the precision of the sensors begins to fail at 30 rpm so the variance in data is more likely to be caused by the sensors than an error with the setup.

The fact that String 1 provides such consistent results between different torques and that it closely approximates its known modulus of rigidity led to the choice of calculating the inherent friction in this system with this data. To accomplish this calculation, the assumption was made that the difference between the ideal and true value of the modulus of rigidity was due to the friction and other torque that would appear in all of the other tests as well. Therefore, to calculate the friction in the system, a solver was utilized to adjust the value of the torque so that the moduli of rigidity would be equal. After this, the difference between the measured torque and the theoretical torque was calculated. This value was then averaged between the various speeds and torques.

However, as mentioned above, certain values of the modulus were less reliable than others. To this end, the values at 30 rpm were discounted due to the high spread associated with the data. Additionally, the data from 10 rpms is less reliable due to the sensors utilized in the setup. Thus, the value utilized for later analysis with friction was the average difference in torque between the ideal values and measured values at 20 rpm. The calculated friction inherent in the system was 0.0124 Nm. This value was utilized later to a great extent, particularly among the smaller strings due to the high ratio of torque provided by friction to the torque provided by the brake.

The second string analyzed was the String 2. This string was the thickest string tested but had a much lower modulus of rigidity than the previous string. As such, it presented less resistance to deformation and thus allowed testing at a greater range of both torque and speed. In addition, the analysis of the data collected from this string will include analysis both with and without the inclusion of the calculated friction.

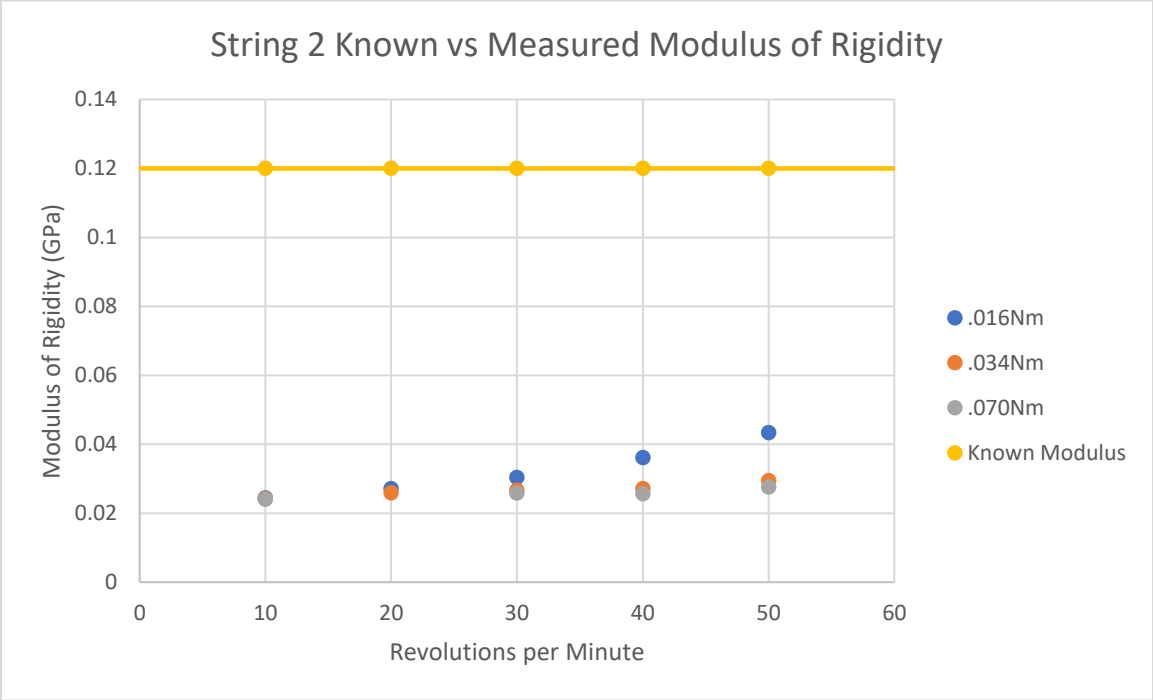

Figure 18: String 2 modulus of rigidity vs revolutions per minute without the inclusion of torque from friction

Figure 18 above shows the measured modulus of rigidity without the inclusion of friction in the calculations. The calculated modulus of rigidity is lower than the known value for the material which indicates that the value of torque is also lower than the true value felt by the string. Therefore, the results that include the calculated friction should be examined as well to determine if they are more accurate.

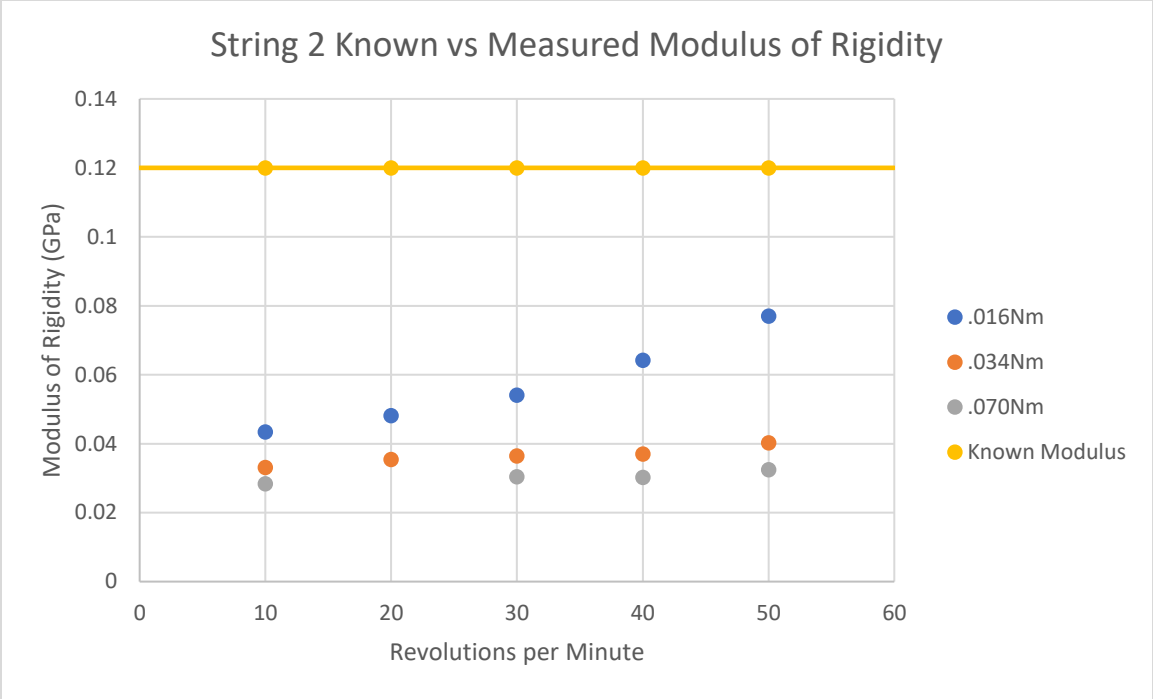

Figure 19: String 2 modulus of rigidity vs revolutions per minute with the inclusion of torque from friction

The inclusion of the torque from the friction serves to bring the values of the modulus of rigidity closer to the values that are to be expected. This indicates that the torque from the system's friction is high enough that it should be included in the results. Therefore, further analysis of this string's validity in testing will include the torque from friction.

The data from this string shows a few things. First, the results for the measured modulus of rigidity are very consistent among the higher torque values. This indicates this string should provide results consistent with the real world. The variation among the datapoints will be discussed below but the apparent increase in the modulus of rigidity for the low torque testing is likely due to the precision of the sensors rather than any failure of the string to provide real data.

The important thing to note for this string is that a very wide range of torque values and speed all produced similar results in terms of the calculated modulus of rigidity. No other tested string was able to provide this range and only String 1 was able to provide the consistency. This indicates that this string setup should be further analyzed as it will likely provide benefits to future testing.

The next analysis is for String 3. This string was much thinner than the two previous strings and as such it did not have the same stiffness that they provided. Because of this, the torque provided by the brake was actually very low compared to the friction provided by the friction inherent in the system. Because of this, the data analysis for this string will include the value of the friction as well as the brake torque.

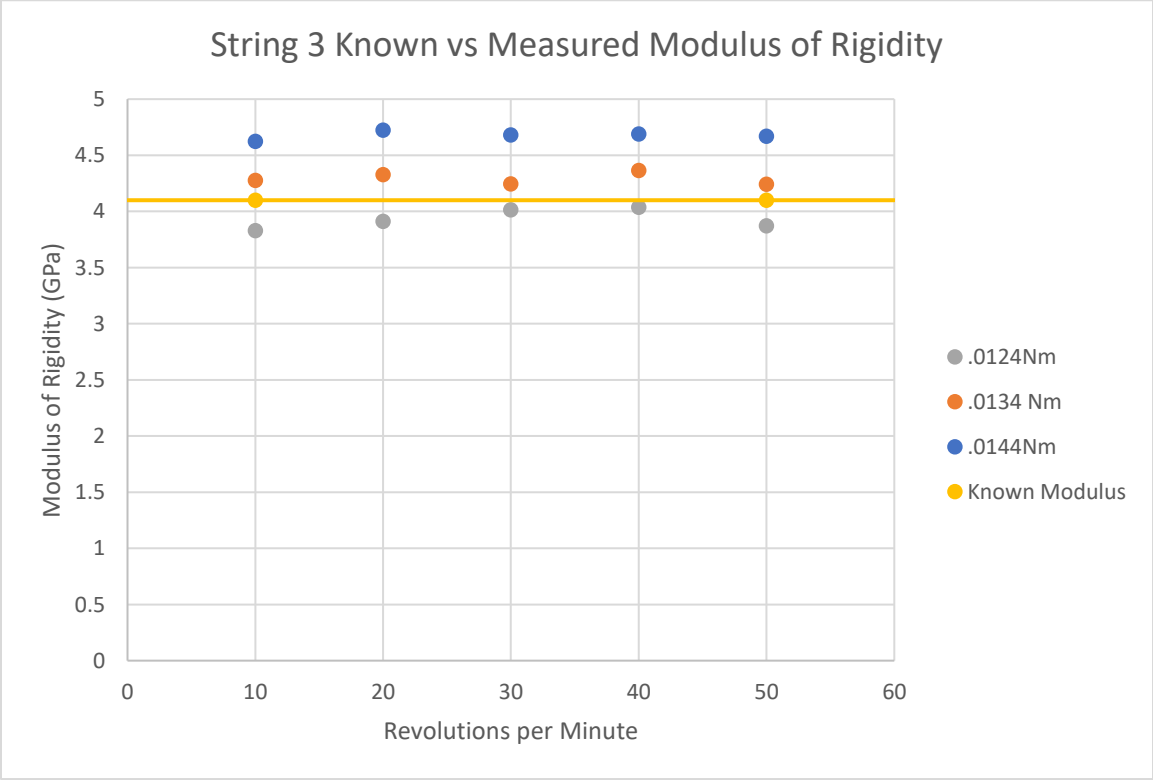

Figure 20: String 3 modulus of rigidity vs revolutions per minute

The modulus of rigidity that was measured for this string is very consistent in its values across the various rpms. This indicates that the data is of good quality. In addition to this, it was able to be tested up to 50 rpms, allowing the analysis of more data than String 1. However, the torque data was based upon the friction from the analysis of String 1's test. Therefore, the value of the calculated modulus of elasticity is more suspect although the consistency of the data occurs regardless of the value of torque.

The calculated values for the modulus of rigidity of String 3 are very similar to the expected value of 4.1 GPa. This indicates that results obtained from the testing not only provided accurate data but that the analysis and estimated values of torque were also very accurate, validating the results obtained earlier from String 1. Therefore, the results obtained from this string should be readily expanded to real-world situations and the testing of parameters on this string should result in applicable result.

This string provided certain, specific challenges. First, its very low stiffness due to its thin cross-section means that very low values of torque must be utilized with it. Second, the maximum value of torque for this string cannot be truly utilized because of the string's brittleness. If the maximum torque for this string's testing were utilized, it would result in a snapping of the string in an unsafe manner and thus must be avoided. These factors serve to limit the practical use of this string even though the data obtained from it was very consistent.

Finally, analysis will be done on String 4. This string, just like the previous one, provided little stiffness compared to the initial two strings due to its low cross-sectional

area. In addition to this, its material construction meant that it too had a low modulus of rigidity which further limited the maximum torque to be utilized in its testing.

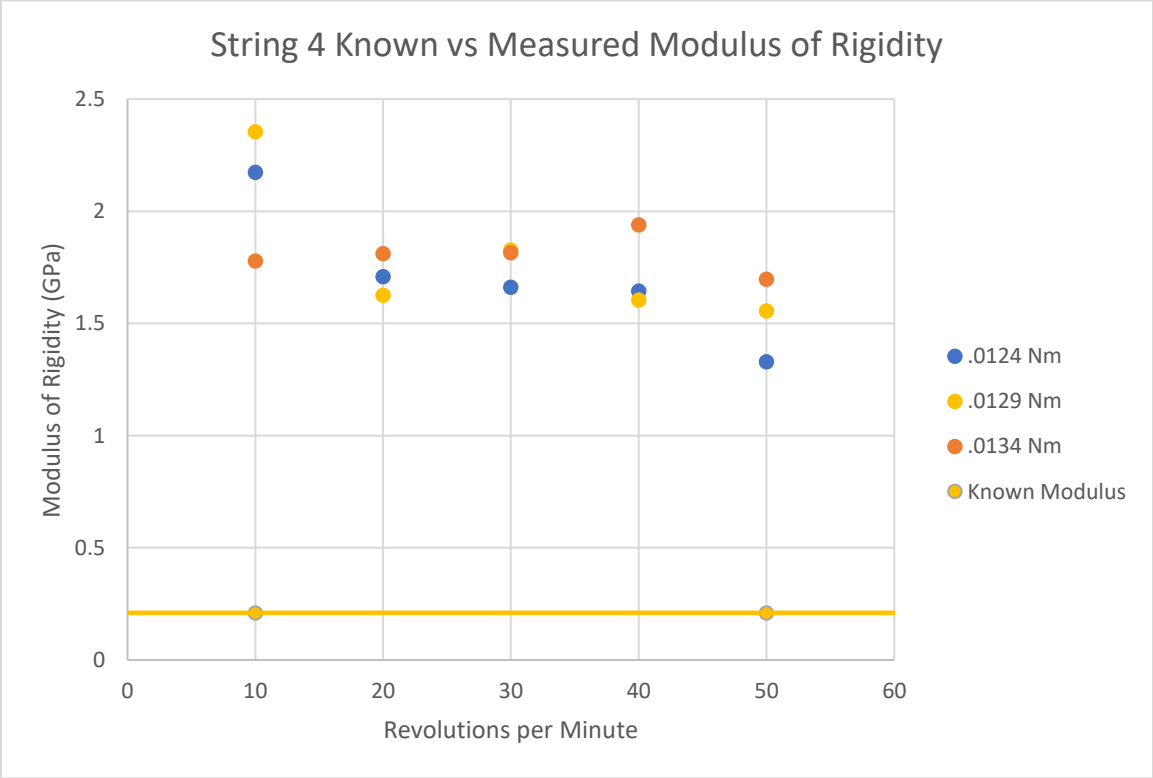

Figure 21: String 4 modulus of rigidity vs revolutions per minute

String 4 is the only string that did not provide consistent results for each set of torque values. As shown in Figure 21 above, the measured value for the modulus of rigidity dropped as the speed increased. This is illogical as it implies that the torque felt by the system decreases with increased speed while in reality the friction should impart additional torque at higher speeds. Therefore, this string had an additional factor impacting the results.

The factor that most likely caused the decrease in the measured value of modulus of rigidity is the deformation and buckling of the string. Additional tests were conducted on this string with higher torque values and the string showed a tendency to

buckle rather than engage in stick-slip interactions. Therefore, this deformation and subsequent change in the torsion constant likely contributed to the error seen.

In addition, this string had calculated values of the modulus of rigidity that were much higher than the expected values. This indicates that the calculated torque was higher than the true value. However, the inconsistency of the base results means that the true difference is not able to be calculated.

6.3 Analysis of Error in the Results and Calculations

The reason to utilize an average value for the results of each torque and speed was the lack of precision from the sensors. Due to their tick rate, the precision was only to the tenth of a second. Therefore, the true value can be anywhere within that range of precision. To analyze how much the data varied with each test, the errors of each torque and speed were calculated. These results are shown below:

RPM	Negative Error	Measured Value	Positive Error
10	0.12	18.10	0.17
20	0.30	22.63	0.40
30	0.20	26.40	0.60

Table 2: Errors from String 1 at 0.057 Nm

RPM	Negative Error	Measured Value	Positive Error
10	0.07	19.23	0.06
20	0.20	22.23	0.07
30	0.40	39.52	0.20

Table 3: Errors from String 1 at 0.064 Nm

RPM	Negative Error	Measured Value	Positive Error
10	0.09	18.98	0.03
20	0.15	22.88	0.13
30	0.20	32.42	0.60

Table 4: Errors from String 1 at 0.070 Nm

The maximum and minimum values for String 1 were typically only a single tick in difference. This means that the precision is as high as can be achieved with the current experimental setup. At the low and medium values rotational speeds, the error is relatively low because the length of each tick is only a fraction of the total time that the sticking occurred. This means that the results can be relied upon. However, once the speed goes to 30 rpms, the error spikes as shown by the error values of 60 percent. At these speeds, the length of sticking is between one and two ticks. Therefore, the difference is fully one hundred percent between the highest and lowest values. This error calls into question whether the results at this speed can be trusted and eliminates the higher speeds as completely unusable. Thus, the fact that the measured modulus of rigidity diverges between torques so much at this speed can be safely assumed to be due to the error from the low sensor tick rate. In addition, the maximum value displayed for the 30-rpm data is the highest value that could even theoretically be detected because it represents the calculated value from a single tick. Therefore, if the data approaches this number, its validity should be further explored.

RPM	Negative Error	Measured Value	Positive Error
10	0.053	0.043	0.092
20	0.086	0.048	0.280
30	0.050	0.054	0.267
40	0.200	0.064	0.200
50	0.200	0.077	0.600

Table 5: Errors from String 2 at 0.016 Nm

RPM	Negative Error	Measured Value	Positive Error
10	0.079	0.033	0.086
20	0.053	0.035	0.014
30	0.080	0.036	0.022
40	0.029	0.037	0.133
50	0.167	0.040	0.250

Table 6: Errors from String 2 at 0.034 Nm

RPM	Negative Error	Measured Value	Positive Error
10	0.060	0.028	0.016
20			
30	0.020	0.030	0.032
40	0.013	0.030	0.057
50	0.083	0.032	0.100

Table 7: Errors from String 2 at 0.070 Nm

When comparing the variation of Strings 1 and 2, both strings typically have about the same variation in actual time, i.e., usually a single tick. However, String 2 spends more time sticking than string 1. This means that the variation between the data is reduced in absolute value and the data for the polyethylene string is therefore more precise. This can be seen in the reduction of percent error for tests conducted with this string. However, String 2 faces the same trouble as String 1 at the lowest torque values. When the applied torque is at its lowest, the length of the sticking at 50 rpm was between one and two tenths of a second. This means that the maximum value shown in the table is again the maximum detectable value. Therefore, values from tests at this torque have a very high error and the results should be scrutinized. In this case, the increase in measured modulus of rigidity values at this lowest torque is likely solely due to the sensors losing precision as the data for the other two torque values did remain consistent at 50 rpms. In addition, for the 50-rpm data at 0.07 Nm of torque, all

datapoints had the same value. Because of this, I extended the range by one tick in either direction to indicate the range of likely values.

RPM	Negative Error	Measured Value	Positive Error
10	0.064	4.63	0.079
20	0.046	4.73	0.073
30	0.076	4.68	0.100
40	0.089	4.69	0.081
50	0.131	4.67	0.158

Table 8: Errors from String 3 at 0.0124 Nm

RPM	Negative Error	Measured Value	Positive Error
10	0.082	4.28	0.127
20	0.093	4.33	0.083
30	0.145	4.25	0.205
40	0.159	4.37	0.289
50	0.163	4.24	0.224

Table 9: Errors from String 3 at 0.0129 Nm

RPM	Negative Error	Measured Value	Positive Error
10	0.094	3.83	0.116
20	0.122	3.91	0.149
30	0.144	4.02	0.323
40	0.165	4.04	0.206
50	0.094	3.87	0.393

Table 10: Errors from String 3 at 0.0134 Nm

Both of the thinner strings suffered from high variance in the data recorded from the sensors. This is particularly the case at 10 rpms. However, the difference between the maximum and minimum is relatively similar because the time of sticking was again much longer than with the thicker strings. This does not hold throughout all of the data though as the variation at the highest rpms increased due to the wide range of results rather than the sensors not being able to precisely record the data. Because of this high error rate in this string, the results gleamed from it should not be held as having the same accuracy as the thicker strings. However, the averages do still follow the expected pattern as discussed above which indicates that the string can still create valid results

with high numbers of tests. These factors should be evaluated when considering this string for use.

RPM	Negative Error	Measured Value	Positive Error
10	0.290	2.17	0.420
20	0.209	1.71	0.265
30	0.133	1.66	0.083
40	0.179	1.64	0.095
50	0.188	1.33	0.083

Table 11: Errors from String 4 at 0.0124 Nm

RPM	Negative Error	Measured Value	Positive Error
10	0.318	2.35	0.364
20	0.136	1.63	0.152
30	0.180	1.83	0.367
40	0.125	1.61	0.167
50	0.278	1.56	0.444

Table 12: Errors from String 4 at 0.0129 Nm

RPM	Negative Error	Measured Value	Positive Error
10	0.125	1.78	0.458
20	0.079	1.81	0.074
30	0.143	1.82	0.071
40	0.248	1.94	0.504
50	0.313	1.70	0.375

Table 13: Errors from String 4 at 0.0134 Nm

Similar to String 3, this string experienced a high variance in recorded values at low speeds. Just as before, this is partly to do with the sensors reducing in accuracy when tested at this speed and the variance does drop once higher speeds are achieved. In fact, above 30 rpms, the data stays within a single tick. Just like before, this factor indicates that the limiting factor on the precision of the data is the tick rate of the sensor and therefore the string provides usable data even if the sensors cannot. However, at the highest rpms, this string has the same issue that the thicker strings had with the length of the sticking being too small in relation to the resolution of the sensors. Unfortunately, just like with String 1, this cannot be fixed through the

application of more torque on the string. The values of torque tested were among the highest that this string could take before buckling. This restricts the value of this string's data at the high end of speeds.

6.4 Analysis of the Strings and Their Suitability for Further Testing

To analyze the various strings, one must first determine if they achieved the objective criteria of providing results that are representative of the real world. To do this, we will review the moduli of rigidity provided by the various strings and their validity.

First, String 1 had a modulus of rigidity that was consistent between the various torque values until the length of sticking became too small to accurately measure. This indicates that the value does reflect the fact that the value of the modulus should not change with torque. However, the value does vary with the rotational speed. This should not happen theoretically. In practice however, this is likely due to the setup itself as the rotary encoders created error at 10 rpms for all samples. In addition, the variation at 30 rpms is due to the low tick rate of the sensors as the precision was not enough to measure the true values of time and therefore the angle of rotation. The test to determine whether or not these errors were enough to make String 1 not suitable for further experimentation was whether the value of torque from friction proved accurate when utilized on String 2. It also proved to be accurate for the analysis of String 3. These factors indicate that the friction calculation based around 20 rpms was accurate. This is particularly important because the value for the true modulus of rigidity for aluminum is

known more exactly than the moduli of rigidity for the other strings. This is due to the fact that the other materials have multiple styles of manufacture and varied chemical makeups that result in a wide range of potential values. What this means in practice is that the results from this string provide the most concrete evidence that the system does represent reality.

However, even if String 1 provides accurate data, should it be utilized in the further testing of stick-slip occurrences and their prevention? The answer to this question is much more subjective. The first consideration is the range of speeds that this string can be tested at. This was the only string that could not be tested above 30 rpms due to its relatively high stiffness. Even at 30 rpms, the results from these tests became unreliable and inconsistent. This is a severe limiting factor. Combined with this, results could only be obtained through the maximum torque values put out by the brake. Additional tests were carried out on this string beyond the ones included in this thesis at a lower torque value, but the results were unusable even at only 10 rpm. There was either no occurrence of stick-slip or lengths of time that were so short as to be undetectable. Because of these limitations, this string is only usable for a narrow range of tests. However, in these tests, this string is reliably gives the most accurate data of any strings tested. Therefore, this string should be utilized in the testing of those conditions but should not be used generally.

The next analysis is on String 2. First, in the objective test, this string remained consistent in the values calculated throughout the various speeds and torque values. In addition to this, the values within each set remained consistent. However, the values at

the lowest brake torque began to vary greatly once high rpms were achieved. This does call into question whether the data obtained from tests with this string are valid. Upon closer examination however, the explanation closely matches that of String 1: the length of sticking becomes short enough that the sensors are unable to properly measure it. Looking at the specific values obtained in the low torque, high rpm tests of this string, the values varied between one and two ticks of data. This means that the error created by the lack of precision is significantly increased. However, the other values obtained from the testing of this string provide very consistent data regardless of the rotational speed which indicates that this string might simply need to be tested with a higher torque value. The accuracy of the values obtained by these experiments is less certain than that of String 1 however due to the range of values for the modulus of rigidity of polyethylene. The uncertainty of this true value does limit the ability of this thesis to ascertain whether these results do match this value but the proof of concept with String 1 indicates that it likely does reflect the true value.

The subjective analysis of this string is more interesting as this string was tested over the greatest range of torques and rotational speeds. In fact, the highest value of torque was nearly three times the lowest value of torque tested. No other string was able to achieve this range of torque values and therefore this string provides fantastic opportunity to simulate many real-world conditions. The control of the conditions on the thicker strings also does grant this string an advantage over the thinner strings as the range of experiments can be known more exactly and chosen rather than forced by the inherent friction of the experimental setup. This also means that the assumption of

the true value of torque provided by the friction of the system is less impactful on the analysis of the results. Additionally, this string will not suffer catastrophic deformation from high torque like both of the thinner strings. This increases the safety of the lab experiments as well as test validity, making this string even more appealing for testing. Due to all of these reasons, this string would make a great candidate for the standard string for testing. By providing accuracy combined with a wide variety of possible test results, this string has capabilities that are unrivaled by the other strings tested in this thesis.

The next analysis will go over String 3. As one of the thinner strings, this string presents some concerns in terms of the accuracy of the analyzed data. In terms of pure data provided by the sensors for this string, this string provides very consistent values of its modulus of rigidity regardless of torque and rotation speed. This makes it a good candidate for testing. However, the potential for error in the analysis of the data appears due to high ratio of torque from the system's friction to the torque from the brake. Because this ratio is so high, much more emphasis must be placed on the friction torque estimation from String 1 than is the case for the thicker strings. However, the results of the calculations do match the known value of nylon's modulus of rigidity so the values of both the raw data and analyzed data are accurate.

The subjective analysis of this string also leaves a bit to be desired. Because of the brittleness of this string, the range of torque values that this string can be tested at is very limited. If the value of torque on this string gets too high, it will shatter which can cause a hazard in the lab and therefore should be avoided as much as possible.

Furthermore, this range is reduced even more by the high value of friction in the current system. These factors severely limit the practicality of this string. The necessity of including friction in the calculations for this string arguably disqualifies it from extensive testing as the torque from the friction is an unknown value and can only be approximated in the current experimental setup. This additional uncertainty reduces the accuracy achievable from the results of this string to a point that the validity of the results cannot be fully ascertained. Therefore, the use of alternative strings is preferred over this string although it will provide accurate and usable results.

Finally, analysis will be done on String 4. This string falls into the category of the thinner strings and thus requires the inclusion of torque from the friction of the system in the calculations. However, after the inclusion of the torque from friction, the values approached the expected values for the modulus of rigidity. Notably though, the behavior of the string's calculated values of its modulus of rigidity follows a pattern unlike any of the other strings. This string is the only one to follow a downward trend as the speed of rotation increases. This fact calls into question the accuracy of the measurements obtained by tests conducted on this string. Even if the value of results for this range of torque and speed values approximates the expected value, future tests with other conditions might not.

Subjectively, this string also struggles. First, similar to the String 3, this string can only operate on a very limited range of torque values. However, unlike that string, the effect of applying too much torque is severe buckling and deformation of the string. While this is preferable to the snapping of the other string, it does present various

issues. First, the deformation will change the structure of the string and thus result in inaccurate results. Second, even when buckling does not occur, the deformation in the string will affect the results of the test. This is likely the cause of the decrease in the calculated modulus of rigidity with an increased speed of rotation. If the string cannot give reliable results at higher speeds, it should not be the standard for experiments and thus this string is not recommended.

To conclude this section, these strings will have various advantages and disadvantages to be considered. First, the usage of the thin strings is discouraged overall due to the importance of the torque from friction. This reliance creates uncertainty that otherwise is not present in the system overall. If the use of a thin string is required for the experiment, then String 3 is recommended because it provides reliable data over the entire tested range of torques and speeds. The usage of String 4 is not recommended due to the errors caused by its deformation. Between the thick strings, String 2 is recommended for general usage in the testing because of the range of both torques and speeds that it can be tested at. String 1 provides good quality data but would not be recommended for general usage due to the limited range of both torque and speed that it can be tested at.

6.5 Improvements to the Experimental Setup

While the results from this experiment indicate that this setup accurately replicates the real world and can thus be utilized for experimentation into stick-slip

occurrence and prevention, there are improvements that can be made that would improve the accuracy and usability of the results.

The first improvement would be to increase the accuracy of the torque measurements by either reducing the friction in the system or by measuring the torque so that an exact value can be added to the brake torque values. Either of these solutions would reduce the uncertainty created by the unknown and high friction in the current experimental setup. In addition to this benefit, reducing the friction in the system would allow a broader range of strings to be utilized. Currently, both of the thin strings tested could only have very low values of torque applied by the brake before significant deformation or destruction of the string occurred. The ability to provide precise and small torque values from the brake would reduce this issue and allow a much greater low range for these strings.

Alternatively, this experiment could benefit by placing a torque sensor on the base of the string. This sensor could bypass the need to determine or reduce the system torque as it would inherently be included in the torque measurement. In addition, this value would increase the accuracy of the torque measurement as it could give an exact value rather than an estimation based upon the chart provided by the brake's manufacturer. This is even more pertinent to the smaller diameter strings as the torque that the brake provides them is not as precisely known as that of the larger strings.

Another improvement to the experimental setup would be a more powerful power supply to increase the top range of torques that the brake could apply to the string. Both Strings 1 and 2 were tested at the maximum torque that the current system

could provide, namely 150 mA or 0.07 Nm. This was particularly limiting for String 1 because even at the highest available torque, the data became unusable beyond 30 rpm. Were higher torque available, the data from 40 or 50 rpms could be usable and thus provide an even better analog for real-world drilling.

The final recommendation to improve the experimental setup is likely the most valuable upgrade. This recommendation is to replace the current rotary encoders with sensors of a higher tick rate. With the current setup, the resolution of the data is only a tenth of a second. This is the greatest limiting factor, especially at the highest rpms. All of the strings had their results averaged between tests of the same speed and torque because the true value of time was between the tenth of a second periods. In addition, many had their maximum variation in data at only one tick. This indicates that a more precise sensor is needed to determine the true value of rotation although the accuracy is still present. Also, any individual test cannot be utilized. Increasing the tick rate would allow the same number of tests to result in five times as many results and increasing the sample size would thereby increase the repeatability of this experiment. Finally, the increase in tick rate would actually mean that the brake's torque would not have to be increased because the data could still be usable with the current torque if the sensors could actually detect the changes in the rotation even with the reduced length of time.

Chapter 7: Conclusion

This study was designed to test the validity of the physical model and the results obtained from it. Based upon the results obtained, the validity has been confirmed. This physical model and the interactions that occur while testing provide accurate information that can then be scaled to real-world drillstrings. This information can then be utilized to determine ways to reduce torsional vibrations and the occurrence of stick-slip interactions.

In addition, this study shows that not all strings will provide the desired results and has thus concluded that further testing should be done with String 2 should the current experimental setup be utilized. However, recommendations were also given that would allow testing with additional strings such as Strings 1 or 3.

The use of this setup can investigate the parameters that will influence the intensity and occurrence of torsional vibrations. Through these tests, analytical models can be physically tested and their results validated, allowing further reduction of stick-slip occurrences and their detrimental effect on drilling. This will further permit successful drilling of wells in a safe and cost-efficient manner and thus improve the state of the industry.

References

Aldred, W.D. and Sheppard, M.C. 1992. Drillstring Vibrations: A New Generation Mechanism and Control Strategies. Presented at the SPE Annual Technical Conference and Exhibition, Washington, District Of Columbia, 4—7 October. SPE-24582-MS. http://dx.doi.org/10.2118/24582-MS.

Ashley, D.K., McNary, X.M., and Tomlinson, J.C. 2001. Extending BHA Life with Multi-Axis Vibration Measurements. Presented at the SPE/IADC Drilling Conference, Amsterdam, Netherlands, 27 February—1 March. SPE-67696-MS. http://dx.doi.org/10.2118/67696-MS.

Baumgart, F. 2000. Stiffness — an unknown world of mechanical science. Injury 31 (2): 14—84. http://dx.doi.org/10.1016/S0020-1383(00)80040-6.

Besaisow, A.A. and Payne, M.L. 1988. A Study of Excitation Mechanisms and Resonances Inducing Bottomhole-Assembly Vibrations. SPE Drilling & Engineering 3 (1): 93—101. SPE-15560-PA. http://dx.doi.org/10.2118/15560-PA.

Brinner, T.R., Traylor, F.T., and Stewart, R.E. 1982. Causes And Prevention Of Vibration Induced Failures In Submergible Oilwell Pumping Equipment. Presented at the SPE Annual Technical Conference and Exhibition, New Orleans, Louisiana, 26—29 September. SPE-11043-MS. http://dx.doi.org/10.2118/.

Dareing, D.W. and Livesay, B.J. 1968. Longitudinal and Angular Drill-String Vibrations With Damping. Journal of Manufacturing Science and Engineering 90 (4): 671—679. http://dx.doi.org/10.1115/1.3604707.

Dareing, D.W. 1984. Drill Collar Length is a Major Factor in Vibration Control. Journal of Petroleum Technology 36 (4): 637—644. SPE-11228-PA. http://dx.doi.org/10.2118/11228-PA.

Dufeyte, M.P. and Henneuse, H. 1991. Detection and Monitoring of the Slip-Stick Motion: Field Experiments. Presented at the SPE/IADC Drilling Conference, Amsterdam, Netherlands, 11—14 March. SPE-21945-MS. http://dx.doi.org/10.2118/21945-MS.

Duleau, A.J.C. 1820. Essai théorique et expérimental sur la Résistance du Fer forgé. Courcier.

Dunayevesky, V.A., Abbassian, F., and Judzis, A. 1993. Dynamic Stability of Drillstrings Under Fluctuating Weight on Bit. SPE Drilling & Completion 8 (2): 84—92. SPE-14329-PA. http://dx.doi.org/10.2118/14329-PA.

Engineering Toolbox. Modulus of Rigidity, https://www.engineeringtoolbox.com/modulus-rigidity-d_946.html(accessed 20 April 2021).

Ertas, D., Bailey, J.R., Wang, L. et al. 2013. Drillstring Mechanics Model for Surveillance, Root Cause Analysis, and Mitigation of Torsional and Axial Vibrations. Presented at the SPE/IADC Drilling Conference, Amsterdam, Netherlands, 5—7 March. SPE-163420-MS. http://dx.doi.org/10.2118/163420-MS.

Esmaeili, A., Elahifar, B., Fruhwirth, R.K. et al. 2012. Laboratory Scale Control of Drilling Parameters to Enhance Rate of Penetration and Reduce Drill String Vibration. Presented at the SPE Saudi Arabia Section Technical Symposium and Exhibition,

Al-Khobar, Saudi Arabia, 8—11 April. SPE-160872-MS. http://dx.doi.org/10.2118/160872-MS.

Higdon, A., Ohlsen, E.H., Stiles, W.B. et al. 1967. Torsional Loading. In Mechanics of Materials, second edition Chapt. 4. New York, New York: John Wiley & Sons, Inc.

Krygier, N., Solarin, A., and Orozova-Bekkevold, I. 2020. A Drilling Company's Perspective on Non-Productive Time NPT Due to Well Stability Issues. Presented at the SPE Norway Subsurface Conference, Virtual, 2—3 November. SPE-200732-MS. http://dx.doi.org/10.2118/200732-MS.

Kyllingstad, A. and Halsey, G.W. 1988. A Study of Slip/Stick Motion of the Bit. SPE Drilling & Completion 3 (4): 369—373. SPE-16659-PA. http://dx.doi.org/10.2118/16659-PA.

Laminated Plastics. Technical Data Sheet High Density Polyethylene, https://laminatedplastics.com/hdpe.pdf(accessed 20 April 2021).

Ledgerwood, L.W., Hoffman, O.J., Jain, J.R. et al. 2010. Downhole Vibration Measurement, Monitoring, and Modeling Reveal Stick/Slip as a Primary Cause of PDC-Bit Damage in Today. Presented at the SPE Annual Technical Conference and Exhibition, Florence, Italy, 19—22 September. SPE-134488-MS. http://dx.doi.org/10.2118/134488-MS.

Lessley, J., Pham, T., and Polk, R. 2017. A Laboratory Analysis of the Kyllingstad and Halsey Pendulum Model with Regards to Stick-Slip Problems.

Omojuwa, E., Osisanya, S., and Ahmed, R. 2012. Integrated Dynamic Analysis for Optimal Axial Load and Torque Transfer in BHAs Used for Extended-Reach

Horizontal Wells. Presented at the SPE Eastern Regional Meeting, Lexington, Kentucky, 3—5 October. SPE-161064-MS. http://dx.doi.org/10.2118/161064-MS.

Patil, P. 2013. Investigation of Torsional Vibrations in a Drillstring Using Modeling and Laboratory Experimentation. Clausthal University of Technology.

Patil, P.A. and Teodoriu, C. 2013. Model Development of Torsional Drillstring and Investigating Parametrically the Stick-Slips Influencing Factors. Journal of Energy Resource Technology. http://dx.doi.org/10.1115/1.4007915.

Santos, H., Placido, J.C.R., and Wolter, C. 1999. Consequences and Relevance of Drillstring Vibration on Wellbore Stability. Presented at the SPE/IADC Drilling Conference, Amsterdam, Netherlands, 9—11 March. SPE-52820-MS. http://dx.doi.org/10.2118/52820-MS.

Sharma, A., Srivastava, S., and Teodoriu, C. 2020. Experimental Design, Instrumentation, and Testing of a Laboratory-Scale Test Rig for Torsional Vibrations—The Next Generation. Energies 13 (18). http://dx.doi.org/10.3390/en13184750.

Spanos, P.D., Sengupta, A.K., Cunningham, R.A. et al. 1995. Modeling of Roller Cone Bit Lift-Off Dynamics in Rotary Drilling. Journal of Energy Resources Technology 117 (3): 197—207. http://dx.doi.org/10.1115/1.2835341.

Westermann, H., Gorelik, I., Rudat, J. et al. 2015. A New Test Rig for Experimental Studies of Drillstring Vibrations. SPE Drilling & Completion 30 (2): 119—128. SPE-176019-PA. http://dx.doi.org/10.2118/176019-PA.

Appendix A: Data Values Obtained from Tests by String

		I	T	L	G			I	T	L	G			I	T	L	G
	Drillstring 1	140	0.057	1.66	27		Drillstring 1	145	0.064	1.66	27		Drillstring 1	150	0.07	1.66	27
		mA	nm	m	Gpa			mA	nm	m	Gpa			mA	nm	m	Gpa
10	rpm						10	rpm					10	rpm			
	0.8	48	0.837758					0.8	48	0.837758				0.9	54	0.942478	
	0.6	36	0.628319					0.7	42	0.733038				0.8	48	0.837758	
	0.7	42	0.733038					0.8	48	0.837758				0.8	48	0.837758	
	0.7	42	0.733038					0.7	42	0.733038				0.8	48	0.837758	
	0.7	42	0.733038					0.7	42	0.733038				0.8	48	0.837758	
	Time (s)	Degree	Rad					Time (s)	Degree	Rad				Time (s)	Degree	Rad	
Average	0.7	42	0.733038				Average	0.74	44.4	0.774926			Average	0.82	49.2	0.858702	
20	rpm						20	rpm					20	rpm			
	0.4	48	0.837758					0.3	36	0.628319				0.4	48	0.837758	
	0.3	36	0.628319					0.3	36	0.628319				0.3	36	0.628319	
	0.2	24	0.418879					0.3	36	0.628319				0.3	36	0.628319	
	0.2	24	0.418879					0.3	36	0.628319				0.3	36	0.628319	
	0.3	36	0.628319					0.4	48	0.837758				0.4	48	0.837758	
	Time (s)	Degree	Rad					Time (s)	Degree	Rad				Time (s)	Degree	Rad	
Average	0.28	33.6	0.586431				Average	0.32	38.4	0.670206			Average	0.34	40.8	0.712094	
30	rpm						30	rpm					30	rpm			
	0.2	36	0.628319					0.1	18	0.314159				0.2	36	0.628319	
	0.2	36	0.628319					0.1	18	0.314159				0.2	36	0.628319	
	0.1	18	0.314159					0.2	36	0.628319				0.2	36	0.628319	
	0.1	18	0.314159					0.1	18	0.314159				0.1	18	0.314159	
	0.2	36	0.628319					0.1	18	0.314159				0.1	18	0.314159	
	Time (s)	Degree	Rad					Time (s)	Degree	Rad				Time (s)	Degree	Rad	
Average	0.16	28.8	0.502655				Average	0.12	21.6	0.376991			Average	0.16	28.8	0.502655	

Table A.1: Data obtained from the testing of String 1

	I	T	L	G			I	T	L	G			I	T	L	G
Drillstring 2	100	0.016	1.695	0.12		Drillstring 2	120	0.034	1.695	0.12		Drillstring 2	150	0.07	1.695	0.12
	mA	nm	m	Gpa			mA	nm	m	Gpa			mA	nm	m	Gpa
10	rpm					10	rpm					10	rpm			
	1.5	90	1.570796				2.8	168	2.932153				6.7	402	7.016224	
	1.3	78	1.361357				3.1	186	3.246312				6.2	372	6.492625	
	1.5	90	1.570796				2.9	174	3.036873				6.2	372	6.492625	
	1.3	78	1.361357				3.1	186	3.246312				6.2	372	6.492625	
	1.5	90	1.570796				3.3	198	3.455752				6.2	372	6.492625	
	Time (s)	Degree	Rad				Time (s)	Degree	Rad				Time (s)	Degree	Rad	
	1.42	85.2	1.487021				3.04	182.4	3.183481				6.3	378	6.597345	
20	rpm					20	rpm					20	rpm			
	0.7	84	1.466077				1.5	180	3.141593				Data Corrupted			
	0.7	84	1.466077				1.4	168	2.932153							
	0.7	84	1.466077				1.4	168	2.932153							
	0.6	72	1.256637				1.4	168	2.932153							
	0.5	60	1.047198				1.4	168	2.932153							
	Time (s)	Degree	Rad				Time (s)	Degree	Rad				Time (s)	Degree	Rad	
	0.64	76.8	1.340413				1.42	170.4	2.974041							
30	rpm					30	rpm					30	rpm			
	0.4	72	1.256637				0.9	162	2.827433				2	360	6.283185	
	0.4	72	1.256637				1	180	3.141593				1.9	342	5.969026	
	0.3	54	0.942478				0.9	162	2.827433				1.9	342	5.969026	
	0.4	72	1.256637				0.9	162	2.827433				2	360	6.283185	
	0.4	72	1.256637				0.9	162	2.827433				2	360	6.283185	
	Time (s)	Degree	Rad				Time (s)	Degree	Rad				Time (s)	Degree	Rad	
	0.38	68.4	1.193805				0.92	165.6	2.890265				1.96	352.8	6.157522	
40	rpm					40	rpm					40	rpm			
	0.2	48	0.837758				0.7	168	2.932153				1.5	360	6.283185	
	0.2	48	0.837758				0.7	168	2.932153				1.5	360	6.283185	
	0.3	72	1.256637				0.7	168	2.932153				1.4	336	5.864306	
	0.2	48	0.837758				0.7	168	2.932153				1.5	360	6.283185	
	0.3	72	1.256637				0.6	144	2.513274				1.5	360	6.283185	
	Time (s)	Degree	Rad				Time (s)	Degree	Rad				Time (s)	Degree	Rad	
	0.24	57.6	1.00531				0.68	163.2	2.848377				1.48	355.2	6.19941	
50	rpm					50	rpm					50	rpm			
	0.2	60	1.047198				0.6	180	3.141593				1.1	330	5.759587	
	0.1	30	0.523599				0.5	150	2.617994				1.1	330	5.759587	
	0.2	60	1.047198				0.5	150	2.617994				1.1	330	5.759587	
	0.2	60	1.047198				0.4	120	2.094395				1.1	330	5.759587	
	0.1	30	0.523599				0.5	150	2.617994				1.1	330	5.759587	
	Time (s)	Degree	Rad				Time (s)	Degree	Rad				Time (s)	Degree	Rad	
	0.16	48	0.837758				0.5	150	2.617994				1.1	330	5.759587	

Table A.2: Data obtained from the testing of String 2

	I	T	L	G			I	T	L	G			I	T	L	G
Drillstring 3	20		1.547	0.12		Drillstring 3	25		1.547	0.12		Drillstring 3	30		1.547	0.12
	mA	Nm	m	Gpa			mA	Nm	m	Gpa			mA	Nm	m	Gpa
10	rpm					10	rpm					10	rpm			
	7.5	450	7.853982				8.2	492	8.58702				9.4	564	9.843657	
	7	420	7.330383				8.6	516	9.005899				10.1	606	10.5767	
	7	420	7.330383				8.3	498	8.69174				9	540	9.424778	
	6.5	390	6.806784				8.2	492	8.58702				9.4	564	9.843657	
	7.1	426	7.435103				8.5	510	8.901179				9.7	582	10.15782	
	7	420	7.330383				7	420	7.330383				7.7	462	8.063421	
	Time (s)	Degree	Rad				7.6	456	7.958701				9.9	594	10.36726	
	7.016667	421	7.347836				7.5	450	7.853982				8.2	492	8.58702	
							8.6	516	9.005899				9.9	594	10.36726	
20	rpm						6.9	414	7.225663				9.7	582	10.15782	
							8	480	8.37758				7.7	462	8.063421	
	3.2	384	6.702064				8.2	492	8.58702				Time (s)	Degree	Rad	
	3.6	432	7.539822				7	420	7.330383				9.154545	549.2727	9.586618	
	3.6	432	7.539822				Time (s)	Degree	Rad							
	3.4	408	7.120943				7.892308	473.5385	8.264805			20	rpm			
	3.5	420	7.330383													
	3.3	396	6.911504			20	rpm						4.7	564	9.843657	
	Time (s)	Degree	Rad										4.9	588	10.26254	
	3.433333	412	7.190757				3.8	456	7.958701				4	480	8.37758	
							4.3	516	9.005899				4.6	552	9.634217	
30	rpm						4	480	8.37758				5	600	10.47198	
							3.6	432	7.539822				4.5	540	9.424778	
	2.4	432	7.539822				3.9	468	8.168141				3.5	420	7.330383	
	2.5	450	7.853982				3.7	444	7.749262				4.6	552	9.634217	
	2.2	396	6.911504				4	480	8.37758				3.9	468	8.168141	
	2.2	396	6.911504				Time (s)	Degree	Rad				5.1	612	10.68142	
	2.4	432	7.539822				3.9	468	8.168141				Time (s)	Degree	Rad	
	2.3	414	7.225663										4.48	537.6	9.38289	
	2.4	432	7.539822			30	rpm									
	2.5	450	7.853982									30	rpm			
	2.1	378	6.597345				2.8	504	8.796459							
	2.1	378	6.597345				3	540	9.424778				2.4	432	7.539822	
	Time (s)	Degree	Rad				2.4	432	7.539822				3	540	9.424778	
	2.31	415.8	7.257079				2.3	414	7.225663				2.2	396	6.911504	
							2.8	504	8.796459				3	540	9.424778	
40	rpm						2.2	396	6.911504				3	540	9.424778	
							2.8	504	8.796459				3.4	612	10.68142	
	1.9	456	7.958701				3.1	558	9.738937				2.4	432	7.539822	
	1.6	384	6.702064				2.8	504	8.796459				3	540	9.424778	
	1.7	408	7.120943				2.2	396	6.911504				3.3	594	10.36726	
	1.8	432	7.539822				2.6	468	8.168141				3.4	612	10.68142	
	1.7	408	7.120943				2.8	504	8.796459				Time (s)	Degree	Rad	
	1.7	408	7.120943				Time (s)	Degree	Rad				2.91	523.8	9.142035	
	1.8	432	7.539822				2.65	477	8.325221							
	1.8	432	7.539822									40	rpm			
	1.6	384	6.702064			40	rpm									
	1.7	408	7.120943										2.1	504	8.796459	
	Time (s)	Degree	Rad				1.7	408	7.120943				1.8	432	7.539822	
	1.73	415.2	7.246607				1.9	456	7.958701				2.2	528	9.215338	
							1.5	360	6.283185				2.3	552	9.634217	
50	rpm						2	480	8.37758				1.9	456	7.958701	
							2.3	552	9.634217				2.6	624	10.89085	
	1.6	480	8.37758				2	480	8.37758				2.4	576	10.0531	
	1.2	360	6.283185				2	480	8.37758				2.3	552	9.634217	
	1.4	420	7.330383				2.2	528	9.215338				2.3	552	9.634217	
	1.4	420	7.330383				2.1	504	8.796459				1.8	432	7.539822	
	1.3	390	6.806784				2	480	8.37758				Time (s)	Degree	Rad	
	1.4	420	7.330383				1.7	408	7.120943				2.17	520.8	9.089675	
	1.5	450	7.853982				1.8	432	7.539822							
	1.4	420	7.330383				Time (s)	Degree	Rad			50	rpm			
	1.3	390	6.806784				1.933333	464	8.098328							
	1.4	420	7.330383										2	600	10.47198	
	Time (s)	Degree	Rad			50	rpm						1.3	390	6.806784	
	1.39	417	7.278023										1.9	570	9.948377	
							1.7	510	8.901179				1.6	480	8.37758	
							1.7	510	8.901179				1.8	540	9.424778	
							1.3	390	6.806784				1.8	540	9.424778	
							1.5	450	7.853982				1.9	570	9.948377	
							1.3	390	6.806784				2	600	10.47198	
							1.7	510	8.901179				2	600	10.47198	
							1.4	420	7.330383				Time (s)	Degree	Rad	
							1.8	540	9.424778				1.811111	543.3333	9.482956	
							1.9	570	9.948377							
							1.8	540	9.424778							
							1.4	420	7.330383							
							Time (s)	Degree	Rad							
							1.590909	477.2727	8.329981							

Table A.3: Data obtained from the testing of String 3

	I	T	L	G			I	T	L	G			I	T	L	G
Drillstring 4	50		1.574	0.12		Drillstring 4	30		1.574	0.12		Drillstring 4	40		1.574	0.12
	mA	Nm	m	Gpa			mA	Nm	m	Gpa			mA	Nm	m	Gpa
10	rpm					10	rpm					10	rpm			
	1.1	66	1.151917				1.4	84	1.466077				0.8	48	0.837758	
	1.4	84	1.466077				1.3	78	1.361357				1	60	1.047198	
	0.9	54	0.942478				1.2	72	1.256637				1.1	66	1.151917	
	1.4	84	1.466077				0.7	42	0.733038				0.7	42	0.733038	
	1.4	84	1.466077				0.8	48	0.837758				1.4	84	1.466077	
	1.5	90	1.570796				0.7	42	0.733038				0.9	54	0.942478	
	1.5	90	1.570796				1.2	72	1.256637				0.8	48	0.837758	
	1.3	78	1.361357				0.9	54	0.942478				1	60	1.047198	
	Time (s)	Degree	Rad				1	60	1.047198				1	60	1.047198	
Average	1.3125	78.75	1.374447				0.7	42	0.733038				0.8	48	0.837758	
							1	60	1.047198				1	60	1.047198	
20	rpm						0.9	54	0.942478				Time (s)	Degree	Rad	
							1.3	78	1.361357			Average	0.954545	57.27273	0.999598	
	0.6	72	1.256637				0.9	54	0.942478			20	rpm			
	0.6	72	1.256637				0.9	54	0.942478							
	0.7	84	1.466077				Time (s)	Degree	Rad				0.7	84	1.466077	
	0.7	84	1.466077			Average	0.99375	59.625	1.040653				0.7	84	1.466077	
	0.7	84	1.466077										0.6	72	1.256637	
	0.6	72	1.256637			20	rpm						0.6	72	1.256637	
	0.7	84	1.466077										0.7	84	1.466077	
	0.6	72	1.256637				0.8	96	1.675516				0.7	84	1.466077	
	0.6	72	1.256637				0.7	84	1.466077				0.8	96	1.675516	
	Time (s)	Degree	Rad				0.6	72	1.256637				Time (s)	Degree	Rad	
Average	0.644444	77.33333	1.349721				0.6	72	1.256637			Average	0.690909	82.90909	1.447037	
							0.6	72	1.256637							
30	rpm						0.5	60	1.047198			30	rpm			
							0.7	84	1.466077							
	0.5	90	1.570796				0.7	84	1.466077				0.5	90	1.570796	
	0.4	72	1.256637				0.5	60	1.047198				0.4	72	1.256637	
	0.4	72	1.256637				0.5	60	1.047198				0.5	90	1.570796	
	0.5	90	1.570796				0.7	84	1.466077				0.4	72	1.256637	
	0.4	72	1.256637				0.7	84	1.466077				0.3	54	0.942478	
	0.4	72	1.256637				0.5	60	1.047198				0.4	72	1.256637	
	0.4	72	1.256637				0.5	60	1.047198				0.3	54	0.942478	
	Time (s)	Degree	Rad				0.7	84	1.466077				0.4	72	1.256637	
Average	0.428571	77.14286	1.346397				0.6	72	1.256637				0.5	90	1.570796	
							0.7	84	1.466077				0.4	72	1.256637	
40	rpm						0.7	84	1.466077				0.3	54	0.942478	
							Time (s)	Degree	Rad				0.4	72	1.256637	
	0.3	72	1.256637			Average	0.632432	75.89189	1.324563				0.5	90	1.570796	
	0.3	72	1.256637										0.4	72	1.256637	
	0.3	72	1.256637										Time (s)	Degree	Rad	
	0.3	72	1.256637			30	rpm					Average	0.41	73.8	1.288053	
	0.3	72	1.256637													
	0.3	72	1.256637				0.4	72	1.256637				0.4	96	1.675516	
	Time (s)	Degree	Rad				0.5	90	1.570796				0.3	72	1.256637	
Average	0.3	72	1.26				0.5	90	1.570796			40	rpm			
							0.4	72	1.256637							
50	rpm						0.4	72	1.256637				0.3	72	1.256637	
													0.4	96	1.675516	
	0.3	90	1.570796				Time (s)	Degree	Rad				0.3	72	1.256637	
	0.3	90	1.570796			Average	0.433333	78	1.361357				0.4	96	1.675516	
	0.2	60	1.047198										0.4	96	1.675516	
	0.4	120	2.094395			40	rpm						0.3	72	1.256637	
	0.2	60	1.047198										0.3	72	1.256637	
	0.3	90	1.570796				0.3	72	1.256637				0.4	96	1.675516	
	0.2	60	1.047198				0.3	72	1.256637				Time (s)	Degree	Rad	
	0.3	90	1.570796				0.3	72	1.256637			Average	0.35	84	1.466077	
	Time (s)	Degree	Rad				0.4	96	1.675516							
Average	0.275	82.5	1.439897				0.3	72	1.256637			50	rpm			
							0.3	72	1.256637							
		Nylon					0.4	96	1.675516				0.3	90	1.570796	
							Time (s)	Degree	Rad				0.3	90	1.570796	
						Average	0.328571	78.85714	1.376317				0.3	90	1.570796	
													0.2	60	1.047198	
						50	rpm						0.3	90	1.570796	
													0.3	90	1.570796	
							0.3	90	1.570796				0.3	90	1.570796	
							0.4	120	2.094395				0.3	90	1.570796	
							0.3	90	1.570796				0.3	90	1.570796	
							0.3	90	1.570796				Time (s)	Degree	Rad	
							0.3	90	1.570796			Average	0.288889	86.66667	1.512619	
							0.4	120	2.094395							
							0.3	90	1.570796							
							0.3	90	1.570796							
							Time (s)	Degree	Rad							
						Average	0.325	97.5	1.701696							

Table A.4: Data obtained from the testing of String 4